Available online at www.sciencedirect.com

ScienceDirect

Advances in Space Research 74 (2024) 2615–2648

ADVANCES IN SPACE RESEARCH (a COSPAR publication)

www.elsevier.com/locate/asr

The Copernicus POD Service

Jaime Fernández [a], Heike Peter [b], Carlos Fernández [a], Javier Berzosa [a], Marc Fernández [a], Luning Bao [a], Miguel Ángel Muñoz [a], Sonia Lara [a], Eva Terradillos [a], Pierre Féménias [c], Carolina Nogueira [d]

[a] GMV AD., Isaac Newton 11. P.T.M. 28760 Tres Cantos, Madrid, Spain
[b] PosiTim UG, In den Löser 15. 64342 Seeheim-Jugenheim, Germany
[c] ESA/ESRIN, Largo Galileo Galilei 1, I-00044 Frascati, Italy
[d] EUMETSAT, Eumetsat Allee 1, 64295 Darmstadt, Germany

Received 29 June 2023; received in revised form 16 February 2024; accepted 27 February 2024
Available online 5 March 2024

Abstract

The Copernicus Precise Orbit Determination (CPOD) Service is in charge of computing the precise orbits and auxiliary data files of the Copernicus Sentinel-1, −2, −3 and −6 missions, using the GPS&Galileo observations obtained on-board. The orbit products and auxiliary data files are provided to the corresponding Payload Data Ground Segments (PDGS) and Payload Data Acquisition and Processing (PDAP) components and to external users through the Copernicus Data Space Ecosystem (CDSE).

The CPOD Service is supported by the CPOD Quality Working Group (QWG), a group of leading experts on GNSS (Global Navigation Satellite System) and POD, which provides independent orbit solutions and techniques to support the quality control (QC) and the validation of the operational products.

The CPOD Service was initially developed in 2013, starting its operational phase in April 2014 after the successful launch of Sentinel-1A. The CPOD Service has accumulated almost 10 years of experience, including its initial development, operations, and periodic evolutions, to the point that currently it is a well-recognized POD Service.

This paper shows in detail the architecture of the CPOD Service, its performance and its evolution over the years, and its future outlook.

Keywords: The European Copernicus Programme; Precise Orbit Determination; Global Navigation Satellite System; Satellite Laser Ranging; Sentinel Satellites

1. Introduction

The European Copernicus programme (Aschbacher and Milagro-Pérez, 2012) consists of several satellite missions dedicated to various remote sensing techniques for observing the planet Earth. The European Commission (EC) manages the Programme, which is implemented in partnership with the European Union (EU) Member States, the European Space Agency (ESA), the European Organisation for the Exploitation of Meteorological Satellites (EUMETSAT), the European Centre for Medium-Range Weather Forecasts (ECMWF), EU Agencies and Mercator Océan.[1] The Copernicus programme provides added value services in the following areas: atmosphere, marine, land, climate change, security and emergency.[2] The provision of these services is based on the processing of environmen-

E-mail addresses: jfernandez@gmv.com (J. Fernández), heike.peter@positim.com (H. Peter), cfernandez@gmv.com (C. Fernández), jberzosa@gmv.com (J. Berzosa), mffernandez@gmv.com (M. Fernández), luning.bao.c@gmv.com (L. Bao), miguel.munoz.t@gmv.com (M.Ángel Muñoz), sonia.lara.espinosa@gmv.com (S. Lara), eva.terradillos.estevez@gmv.com (E. Terradillos), Pierre.Femenias@esa.int (P. Féménias), carolina.nogueiraloddo@eumetsat.int (C. Nogueira).

[1] https://www.copernicus.eu/en/about-copernicus.
[2] https://www.copernicus.eu/en/copernicus-services.

https://doi.org/10.1016/j.asr.2024.02.056
0273-1177/

tal data collected from Earth observation satellites (Copernicus Sentinels) and in situ sensors.

The Copernicus Sentinels are divided into missions. Among them Sentinel-1, −2, −3 and −6 (Torres et al., 2012; ESA Sentinel-2 team, 2012; ESA Sentinel-3 team, 2012; Donlon et al., 2021) are dedicated satellite missions with optical or radar instruments for dedicated Earth observation tasks, while Sentinel-4 and −5 (Stark et al., 2020; Veefkind et al., 2012) are instruments onboard EUMETSAT´s weather satellites. The Copernicus expansion programme will add new missions to this family in the future.

The CPOD Service is one of the Copernicus services. The service was envisioned by ESA to give the European industry the full responsibility of generating precise orbit products of the Copernicus Sentinel missions that require these products. Historically, LEO (Low Earth Orbit) POD was developed by space agencies including ESA, NASA (National Aeronautics and Space Administration), CNES (Centre Nationale d'Etudes Spatiales), DLR (Deutsches Zentrum für Luft- und Raumfahrt), universities and research institutions, e.g., in Europe, AIUB (Astronomical Institute University of Bern), GFZ (GeoForschungsZentrum), TU Munich (TUM), and TU Delft (TUD).

The CPOD Service has a clear goal, which is the operational and on time provision of precise orbit products and other auxiliary files to the corresponding Payload Data Ground Segments (PDGS) / Payload Data and Acquisition Processing (PDAP) to support the generation of the Sentinel missions core science user products, and to distribute them to the user community. Examples of applications that need POD include SAR (Synthetic Aperture Radar), Interferometry-SAR, and Altimetry. Satellite observation data needed for POD and the products are also provided to the user community via the CDSE.[3] The first contract for the CPOD Service was signed in 2013 to start preparatory work; the service became operational with the launch of the first satellite Sentinel-1A in April 2014.

Precise orbit products for European Earth observation satellites have already been provided for previous ESA missions by single institutions or universities, e.g., within the GOCE (Gravity Field and Steady-State Ocean Circulation Explorer) High-level Processing Facility (Floberghagen et al., 2011; Visser et al., 2009; Bock et al., 2014) or within the Swarm Instrument Processing Facility (Friis-Christensen et al., 2008; van den IJssel et al. 2015). Different to these two mentioned facilities the CPOD Service is a consortium led by a company (GMV, Spain), which is also responsible for the operations of the service. It is much more complex regarding the number of missions and satellites processed and regarding the requirements on latency and accuracy (Table 3) than other previous POD services. The requirements range from very short latency of 10 min for the Sentinel-3 (S-3) and Sentinel-6 (S-6) Near Real Time (NRT) orbit product to a very high accuracy of 2 cm in radial component for the S-3 Non-Time Critical (NTC) orbit products.

In addition to GMV, the consortium includes an external GNSS product provider (EGP) needed for the NRT and the Short-Time Critical (STC) orbit production and several additional members from industry, universities, and research organizations. In addition, the service is accompanied by the Copernicus POD Quality Working Group (QWG) chaired by ESA, co-chaired by EUMETSAT and consisting of experts in LEO POD, altimetry and GNSS receiver technology.

The Sentinel satellite orbit products from the CPOD Service rely on GNSS-based POD. Until January 2023 NAPEOS (Navigation Package for Earth Observation Satellites, Springer et al., 2011) was used for operations. End of January 2023 the CPOD Service switched to the GMV in-house developed software package ***FocusPOD*** (Fernández et al., 2023). The reduced-dynamic orbit determination technique is applied (Wu et al., 1991) based on the Precise Point Positioning (PPP; Zumberge et al., 1997) approach. All processed Copernicus satellites are equipped with two redundant GPS (all currently flying Sentinel-1, −2, and −3 satellites) or two redundant GPS and Galileo (Sentinel-6 Michael Freilich (MF)) observation units. The Sentinel-3 and the Sentinel-6 MF satellites are also equipped with a DORIS (Doppler Orbitography and Radiopositioning Integrated by Satellite, Debaisieux et al., 1985) receiver and a laser retro reflector (LRR) array for Satellite Laser Ranging (SLR; Pearlman et al., 2019). The availability of these two other space geodetic observation techniques, SLR and DORIS, allows for independent orbit accuracy validation of the GNSS-based orbit products. Sentinel-6 MF even carries an additional GPS POD antenna, which is connected to a GNSS-RO (radio occultation) receiver being one of the scientific instruments onboard the satellite. Comparisons with orbit products based on the observations from these additional POD instruments is an important asset of the Sentinel-6 MF mission.

For all satellites, orbit accuracy is validated based on comparisons to a combined orbit solution. This combined orbit solution is a weighted mean of orbit solutions (Beutler et al., 1995; Fernández et al., 2022) provided by members of the CPOD QWG (based on different software packages and different orbit parametrization schemes) on a regular basis to the CPOD Service. In the case of Sentinel-1 (S-1) and Sentinel-2 (S-2) this is the only possibility to assess the orbit accuracy although it is not based on an independent observation technique. The results of this quality control are summarized in Regular Service Review (RSR) reports available on the Sentinel online website.[4] The RSR results confirm the excellent performance of the operational orbit products of the service.

[3] https://dataspace.copernicus.eu/.

[4] E.g. https://sentinels.copernicus.eu/web/sentinel/technical-guides/sentinel-3-altimetry/pod/documentation

The CPOD Service has now been running operationally for more than nine years. The unique setup of the service in strong connection and cooperation with the CPOD QWG led to an extremely valuable and constructive exchange on challenges and enhancements of LEO POD. Significant improvements of the CPOD orbit products could be reached as well as of the orbit products from the CPOD QWG members. Several studies and publications from CPOD Service and CPOD QWG members accompanied the positive development of the CPOD Service, which also confirms that the service closely follows state-of-the-art LEO POD procedures.

First publications concentrated on the technical and organisational setup of the service (Fernández et al., 2014, 2015a; Peter et al., 2015) and first operational results (Fernández et al., 2015b, 2016). Investigations on radial offsets between the different CPOD QWG orbit solutions for the first satellite Sentinel-1A (Peter et al., 2017) led to a correction of the z-component (radial) of the GPS antenna phase center offset (PCO) by 29 mm not only for Sentinel-1A but for all currently flying Sentinel-1, −2 and −3 satellites. Significant differences in the metrics of the two identically built Sentinel-1 satellites revealed a misunderstanding of the technical documentation and the antenna reference point (ARP) coordinates had to be corrected (Fernández et al., 2022). Furthermore, a deeper analysis of the impact of the satellite macro model, orbit parametrization and observation modelling on antenna offset estimation has been performed (Peter et al., 2020). An improved macro model with simple assumptions on shadowing effects has been developed throughout this analysis. The switch to the new ARP coordinates made a reprocessing of the Sentinel-1A and −1B orbits necessary, leading to a consistent improved time series of orbits for the entire mission time of both satellites (Fernández et al., 2022). Major but not the only updates in the orbit processing during the years have been an update of the orbit parametrization (Peter et al., 2021) and the switch to integer ambiguity resolution (IAR), as shown in Jäggi et al. (2007), Laurichesse et al. (2009) and Bertiger et al. (2010), can bring substantial improvements in the precision and accuracy. This has been shown for the first time for one of the Sentinel satellites (Sentinel-3A) by Montenbruck et al. (2018), from DLR, a CPOD Service and CPOD QWG member. In this same work, a bias of 10 mm in the cross-track direction was identified, probably due to an incorrect definition of the centre of mass (CoM) of the satellite. Sentinel-3A orbit validation results from the first mission years have been presented in (Fernández et al., 2019). Sentinel-3B has been the first satellite tracking GPS L2C signals on the redundant receiver during commissioning phase. First results have been presented in Berzosa et al. (2021).

AIUB, being also a member of the CPOD Service and the CPOD QWG implemented the dedicated non-gravitational force modelling for LEO POD (Mao et al., 2021) into the Bernese GNSS Software (Dach et al., 2015) to be able to perform a more dynamic orbit determination for LEOs than before (Jäggi et al., 2006). The handling of manoeuvres for LEOs has also been improved at AIUB (Mao et al., 2023). In addition, an alternative approach to combine precise orbit solutions has been presented by Kobel et al. (2019). The CPOD QWG member TUM compared different GPS satellite bias products for integer ambiguity fixing for Sentinel-3 POD (Duan and Hugentobler, 2021). Montenbruck et al. (2021) showed for the first time the performance of precise orbit determination using a combined GPS/Galileo receiver on-board Sentinel-6A.

Studies with very close connection to the CPOD Service are the application of newly generated COST-G (Combination Service for Time-variable Gravity Fields, Jäggi et al., 2020) FSMs (Fitted Signal Models) for LEO POD to improve the modelling of the time-variable gravity signal (Peter et al., 2022) and the estimation of SLR station range biases based on multi-LEO precise orbits (Saquet et al., 2024). Rudenko et al. (2023) included the operational CPOD Service Sentinel-3A and −3B NTC orbit solutions in their assessment of radial orbit errors of altimetry satellites based on several available orbit time series. Conrad et al. (2022) developed two improvements in solar radiation pressure (SRP) modelling for Sentinel-6A which could be considered for future evolutions of the CPOD Service.

Although the list of publications connected to the CPOD Service is already quite long a detailed overview of the service itself, the organisational setup, major changes, enhancements, and performance over the long operational time have not been given. This article aims to fill this gap. Section 2 briefly presents information about the Copernicus Sentinel missions processed by the CPOD Service. Section 3 gives a detailed description of the organisational and technical setup of the service and the major changes throughout the years. Section 4 present an assessment of the quality of the different orbit products over the history of the CPOD Service. Finally, Section 5 gives the conclusions and outlook.

2. Description of Copernicus satellite missions

2.1. Copernicus Sentinel-1 mission

Until now the Copernicus Sentinel-1 mission (Fig. 1) is composed of two satellites (as of today A & B units), carrying a C-band SAR, that continues gathering SAR data by European Remote Sensing (ERS) (ESA, 1992) and Envisat (Louet, 2001) missions. Sentinel-1A was launched

Fig. 1. Artist's rendition of the deployed Sentinel-1 spacecraft (image credit: ESA/ATG medialab).

on 03 April 2014 while Sentinel-1B was launched on 25 April 2016. This mission is controlled from the European Space Operation Centre (ESOC) in Darmstadt, Germany. At the time of writing this paper, Sentinel-1A is still in good health, but Sentinel-1B was declared out of mission on 23 December 2021 due to an anomaly which prevents the use of the radar, although the satellite still remains in orbit under control by the Flight Operation Segment (FOS). A third satellite (Sentinel-1C) is foreseen to be launched not before Q4 2023, which will substitute the failed Sentinel-1B. A fourth satellite (Sentinel-1D) is intended to be launched in the time period 2024–2028.

The Sentinel-1 satellites orbit in a Sun-synchronous near-circular dawn-dusk orbit, with a mean altitude of 693 km, and an inclination of 98.18°. The orbital period is roughly 98.6 min, and the ground track repeat cycle is 12 days (accumulating 175 orbits per cycle). Both satellites are 180° out of phase.

The Sentinel-1 satellites follow a Zero-Doppler steering and a roll steering. The solar panel is fixed with respect to the body of the spacecraft, so it is not rotating to optimize the angle with respect to the Sun.

The Sentinel-1 satellites are equipped with two, dual-frequency, geodetic grade GPS/GNSS receivers. The A & B units are equipped with a GPS-only receiver (Zangerl et al., 2014) tracking the legacy C/A, P1 & P2 signals; the B unit is also capable of tracking the GPS L2C-M signal, although it has been used only for testing. The C & D units will be equipped with a GPS + Galileo receiver capable of tracking not only the GPS legacy signals, but also GPS L2C and L5, and Galileo E1 and E5a. The Sentinel-1 GNSS data is downlinked several times per orbit (through the Svalbard, Matera and Maspalomas tracking stations, and also through the European Data Relay Satellite (EDRS[5]) using an optical link. The GNSS data as well as attitude quaternions are made available to the CPOD Service to generate the precise orbit products.

The operational Sentinel-1 orbit products generated by the CPOD Service include:

- Predicted orbit files in NRT (available before SAR data take acquisition).
- Restituted orbit files in NRT.
- Precise Orbit Ephemeris (POE) in Non-Time Critical (NTC), to support interferometry
- GNSS L1B RINEX (Romero, 2020) products.
- Auxiliary data files (e.g., attitude quaternions).

2.2. Copernicus Sentinel-2 mission

Until now the Copernicus Sentinel-2 mission (Fig. 2) is also composed of two satellites (as of today A & B units), carrying a Multi-Spectral Instrument (MSI) with optical and infrared sensors that provide enhanced continuity of data so far provided by SPOT-5[6] (Satellite Pour l'Observation de la Terre) and Landsat-7[7] missions. Sentinel-2A was launched on 23 June 2015, and Sentinel-2B was launched on 07 March 2017. This mission is controlled from ESOC as well. At the time of writing this paper, both satellites are in good health. A third satellite (Sentinel-2C) is foreseen to be launched not before 2024 to replace one of the

[5] https://www.eoportal.org/satellite-missions/edrs.
[6] https://www.eoportal.org/satellite-missions/spot-5.
[7] https://www.eoportal.org/satellite-missions/landsat-7.

Fig. 2. Artist's rendition of the deployed Sentinel-2 spacecraft (image credit: ESA/ATG medialab).

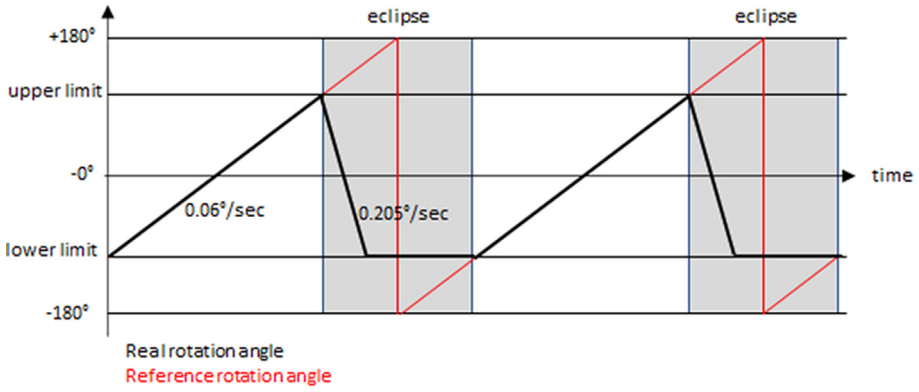

Fig. 3. Representation of Sentinel-2 rotation angle of solar array.

flying units (A or B). The fourth satellite (Sentinel-2D) is intended to be launched in the time period 2025–2028.

The Sentinel-2 satellites orbit in a Sun-synchronous near-circular orbit, with a mean altitude of 786 km, and an inclination of 98.6°. The orbital period is roughly 100.6 min, and the ground track repeat cycle is 10 days (accumulating 143 orbits per cycle). Both satellites are 180° out of phase, so the revisit time of the constellation is 5 days. Sentinel-2 also downlink the data as Sentinel-1, with three ground stations and through the EDRS system.

The Sentinel-2 satellites follows a yaw-steering guidance. The solar panel rotates to optimize the exposure to the Sun (at 0.06°/sec), but it will rewind as soon as the satellite enters the eclipse phase (at 0.205°/sec) (see Fig. 3).

Beyond the main MSI the Sentinel-2 satellites are equipped with two dual-frequency GNSS receivers (relying on GPS constellation signals only for the A & B units and compatible with both GPS and Galileo for the following C & D units) for the generation of the operational orbit products.

The operational Sentinel-2 orbit products generated by the CPOD Service include:

- Predicted orbits files in NRT (discontinued after January 2023)
- Restituted orbit files in NRT.
- GNSS L1B RINEX products.
- Auxiliary data Files (e.g., attitude quaternions).

2.3. Copernicus Sentinel-3 mission

The Copernicus Sentinel-3 mission (Fig. 4) is composed of two satellites (as of today A & B units) as well, carrying several sensors: i) An Ocean and Land Colour Imager (OLCI), ii) a Sea and Land Surface Temperature Radiome-

Fig. 4. Artist's rendition of the deployed Sentinel-3 spacecraft (image credit: ESA/ATG medialab).

ter (SLSTR), iii) a SAR Radar Altimeter (SRAL), iv) a Microwave Radiometer (MWR) to support SRAL. This suite of instruments continues the generation of the products from the Envisat and ERS missions. Sentinel-3A was launched on 16 February 2016 while Sentinel-3B was launched on 25 April 2018. The mission is controlled by EUMETSAT in Darmstadt, Germany, although the Launch and Early Orbit phase (LEOP) was done by ESOC. At the time of writing this paper, both satellites are in good health. A third satellite (Sentinel-3C) is foreseen to be launched not before Q4 2024, to replace one of the flying units (A or B). A fourth satellite (Sentinel-3D) is intended to be launched in the time period 2025–2028.

The Sentinel-3 satellites orbit in a Sun-synchronous near-circular orbit, with a mean altitude of 807 km, and an inclination of 98.65°. The orbital period is roughly 101 min, and the ground track repeat cycle is 27 days (accumulating 385 orbits per cycle); the revisit time is less than or equal to four days (varies with latitude). Both satellites are 140° out of phase (contrary to Sentinel-1 and −2 for which it is 180°), to measure ocean features such as eddies as accurately as possible.[8] Sentinel-3 downlinks data only from Svalbard station in Norway once per orbit.

The Sentinel-3 satellites follows a geodetic pointing with yaw-steering guidance. The solar panel rotates to optimize the exposure to the Sun.

The POD payload for the Sentinel-3 satellites includes the same GPS/GNSS receiver as Sentinel-1 and −2 (see above), but it is complemented with two other payloads: a DORIS instrument and a Laser Retro-reflector Array (LRA). Sentinel-3 is also equipped with an Ultra-Stable Oscillator (USO), which provides the time signal to the SRAL, GPS/GNSS and DORIS instruments.

The operational Sentinel-3 orbit products generated by the CPOD Service include:

- Restituted Orbit Files in NRT, to support NRT L2 SRAL/MWR processing in less than 3 h from sensing.
- Medium Orbit Ephemeris (MOE) in STC, to support STC L2 SRAL/MWR processing in less than 48 h from sensing.
- Precise Orbit Ephemeris[9] (POE) in Non-Time Critical (NTC), to support the NTC L2 SRAL/MWR processing in less than 1 month from sensing.
- Preliminary and Precise Platform Auxiliary Data Files.
- GNSS L1B RINEX products.
- Auxiliary data files (e.g., attitude quaternions).
- Predicted orbits, in the Consolidated Prediction Format (CPF), to support the SLR tracking by the International Laser Ranging Service (ILRS).

2.4. Copernicus Sentinel-6 mission

The Copernicus Sentinel-6 mission (Fig. 5) is currently composed of a single satellite (Sentinel-6 Michael Freilich (MF)), that is built on heritage from the Jason series of ocean topography satellites and from ESA's CryoSat mission, and it is designed to complement ocean information from Sentinel-3. Sentinel-6 MF carries three main instruments: i) the Poseidon-4 (POS4) SAR altimeter, ii) the Advanced Microwave Radiometer for Climate (AMR-C), and iii) the High-Resolution Microwave Radiometer (HRMR). Sentinel-6 MF was launched on 21 November 2020. This mission is controlled by EUMETSAT. On 7 April 2022 the satellite took over the role as reference altimeter satellite from Jason-3. At the time of writing this

[8] https://www.eoportal.org/satellite-missions/copernicus-sentinel-3#status-of-project-development.

[9] The operational Sentinel-3 MOE and POE are generated by CNES. The solution from CPOD Service is the back-up.

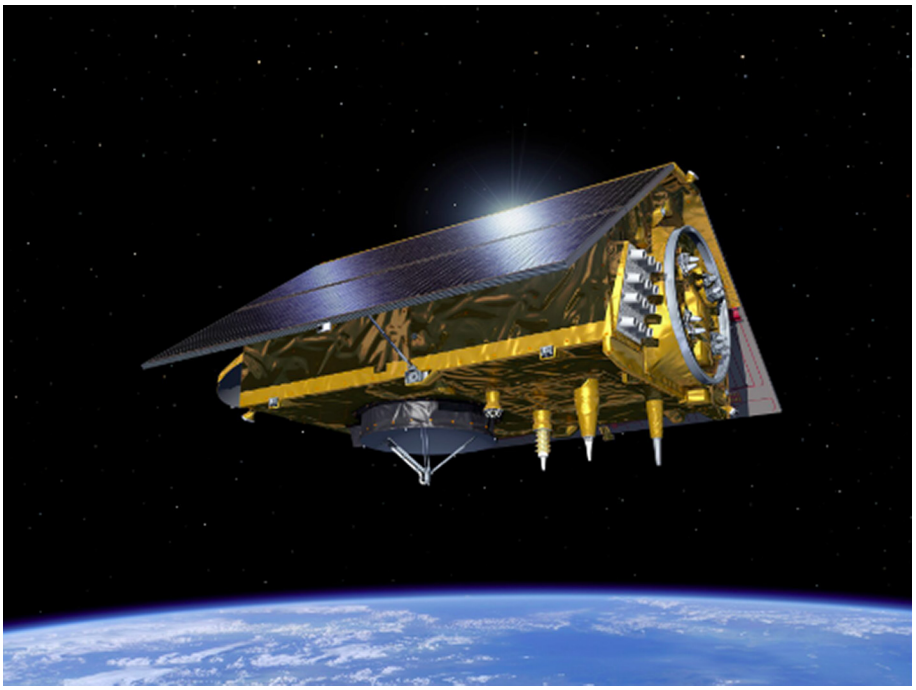

Fig. 5. Sentinel-6 (Image Credit: European Space Agency).

paper, the satellite is in good health. A second satellite (Sentinel-6B) is foreseen to be launched not before Q4 2025, to be operated along with Sentinel-6 MF and to take over as reference altimeter satellite after successful commissioning and tandem phase.

Sentinel-6 MF satellite is in a non-Sun-synchronous near-circular orbit, with a mean altitude of 1336 km, and an inclination of 66°. The orbital period is roughly 112.4 min, and the ground track repeat cycle is 9 days and 22 h.

The Sentinel-6 MF satellite follows a geodetic pointing with yaw-steering guidance. The solar panels are attached to the body of the spacecraft, so they do not rotate, and indeed, they shadow the lower side of the spacecraft, complicating the modelling of the solar radiation pressure.

The POD payload for the Sentinel-6 satellites includes a GPS + Galileo receiver (same characteristics as those described for the C & D units of Sentinel-1), but it is complemented with two other instruments as for Sentinel-3: a DORIS receiver and an LRA. Additionally, it is equipped with a GNSS Radio-Occultation instrument provided by NASA.

The operational Sentinel-6 orbit products generated by the CPOD Service include:

- Restituted Orbit Files in NRT, to support NRT L2 altimetry processing in less than 3 h from sensing
- GNSS L1B RINEX products.
- Auxiliary data files (e.g., attitude quaternions).

2.5. GNSS payload on Copernicus Sentinel

All the Sentinels missions described in this paper incorporate two dual-frequency GNSS receivers developed by RUAG Space, Austria. The Sentinel-1, −2, and −3 A &

Table 1
Observation types tracked by the GNSS receivers.

Constellation	Code	RINEX	AGGA	GNSS Blocks	Mission	Code
GPS	L1 C/A	1C	2 / 4	ALL	ALL	
	L1 P(Y)	1 W	2	IIR, IIR-M, IIF, III	ALL	Semi-codeless
	L2 P(Y)	2 W	2	IIR, IIR-M, IIF, III	ALL	Semi-codeless
	L2-CM	2S	2	IIR-M, IIF, III	S-1,2,3B units	Moderate
	L2-CL	2L	4	IIR-M, IIF, III	S-6	Long
	L5-Q	5Q	4	IIF, III	S-6	Pilot
Galileo	E1-C	1C	4	ALL	S-6	BOC (1,1) pilot
	E5-Q	5Q	4	ALL	S-6	Pilot

Table 2
Operational configuration of GNSS receivers on-board Sentinels.

Constellation	GNSS Blocks	Sentinel-1, 2, 3	Sentinel-6
GPS	IIR	L1 C/A, P(Y)	L1 C/A, P(Y)
	IIR-M	L1 C/A, P(Y)	L1 C/A, L2C
	IIF	L1 C/A, P(Y)	L1 C/A, L2C
	III	L1 C/A, P(Y)	L1 C/A, L2C
Galileo	ALL	n/a	E1-C, E5-Q
	ALL	n/a	E1-C, E5-Q

B units incorporate a GPS receiver, while Sentinel-6A MF incorporates the new PODRIX GPS + Galileo receiver. Table 1 shows the GNSS observations tracked and the corresponding RINEX (Romero, 2020) identifiers. It also shows the Advanced GPS/GLONASS ASIC (AGGA) chip in charge of the tracking of each code. The GPS receiver on-board Sentinel-1, −2, and −3 A&B satellites incorporates an AGGA-2 chip (Roselló et al., 2012) with 3 x 8 channels for tracking the civil L1 C/A and the military P(Y)-code, that allow tracking up to 8 GPS satellites simultaneously. Sentinel-6 MF incorporates both, an AGGA-2 and the new AGGA-4 chip with 36 single frequency channels that allow for tracking up to 18 satellites in two frequencies, which is used for tracking the GPS L2-CL, L5-Q and Galileo codes (Table 2).

The GPS receiver on-board Sentinel-1, −2, and −3 A units allows for just one configuration, tracking L1 C/A, and P(Y). The B units can optionally track the L2-CM code, instead of P(Y) for GPS satellites of Block IIR-M, IIF and III; this mode has only been used experimentally in Sentinel-3B between 11th and 15th of June 2018 (Berzosa et al., 2021). The new PODRIX receiver, on-board Sentinel-6 MF, has multiple potential configurations for GPS, allowing tracking only P(Y), or to track L2-CL and / or L5-Q with those GPS satellites transmitting them. Multiple tracking configurations were tested on Sentinel-6 MF between November 2020 and March 2021, as part of the commissioning phase.

Fig. 6 shows in the left image, the GPS channel occupancy, per tracked code, for Sentinel-3A, on 2022/09/01. The maximum number of channels here is 8, as mentioned above. On the right-hand side, it is represented the C/N0 vs. elevation of the three codes. The bigger losses at low elevations of the S2W are due to the use of semi-codeless tracking schemes that suffer from signal-strength-dependent squaring losses (Woo, 2000; Montenbruck et al., 2006). Similar plots can be obtained for Sentinel-1, −2 and −3.

Fig. 7 shows on the top image, the GNSS channel occupancy, per tracked code, for Sentinel-6A on 2022/09/01. Due to the different tracking for GPS P(Y) (only tracked for GPS Block IIR), than for the other codes (of GPS blocks IIR-M, IIF and III), the channel distribution is asymmetric. The images below represent the C/N0 vs. elevation of the different codes.

Table 3
Characteristics of the products generated by CPOD Service.

Product Type	Description	Type	File Type	S-1	S-2	S-3	S-6	Timeliness	Accuracy[10]
POD Orbit Files	Predicted Orbit File	NRT	AUX_PREORB	X				30 min	S1: 1 m (3D)
									S2: 3 m (3D)
	Restituted Orbit File	NRT	AUX_RESORB	X	X			30 min	S1: 10 cm (3D)
									S2: 1 m (3D)
	Medium Orbit Ephemerides (MOE) Orbit File	STC	AUX_MOEORB			X		48 h	3 cm (radial)
	Precise Orbit Ephemerides (POE) Orbit File	NTC	AUX_POEORB	X		X		S1: 20 d	S1: 5 cm (3D)
								S3: 25 d	S3: 2 cm (radial)
	NRT Restituted Orbit Ephemeris	NRT	ROE_AX			X		10 min	8 cm (radial)
	NRT Restituted Orbit Ephemeris	NRT	AX___ROE__AX				X	10 min	5 cm (radial)
Auxiliary Files for Sentinels	Attitude Restituted Data[11]	NRT	AUX_RESATT	X				n/a	n/a
	Preliminary Platform Data File	STC	AUX_PRLPTF			X		48 h	n/a
	Precise Platform Data File	NTC	AUX_PRCPTF			X		25 d	n/a
	NRT Platform Data File	NRT	SR_2_NRPPAX			X		10 min	n/a
GNSS L1b RINEX files	Hourly GNSS L1b RINEX File	NRT	AUX_GNSSRX			X		10 min	n/a
	Daily GNSS L1b RINEX File	STC	AUX_GNSSRD			X		3 days	n/a
	Daily GNSS L1b RINEX File	STC	AUX_GNSSRD	X	X	X	X	7 days	n/a
	Hourly GNSS RINEX File	NRT	GN_1B_RNXH_AX				X	10 min	n/a
	Daily GNSS RINEX File	STC	GN_1B_RNXD_AX				X	3 days	n/a
Quaternions Files	Processed Quaternions Files	STC	AUX_PROQUA	X	X	X	X	7 days	n/a
CPF predictions	CPF orbit predictions	STC	AUX_STCCPF			X		n/a	n/a

[10] Original requirement from the respective mission requirement documents
[11] Not generated for the moment.

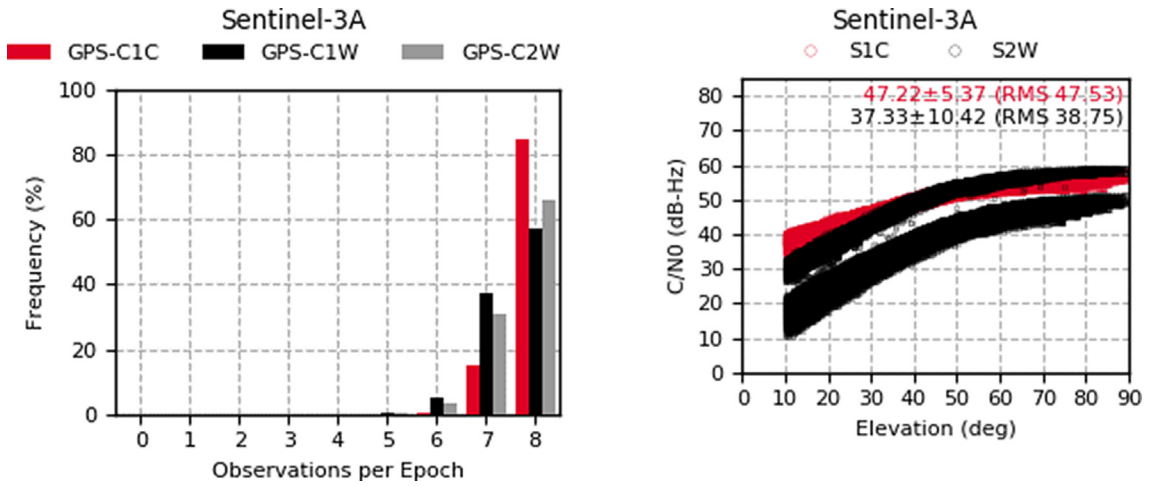

Fig. 6. Channel occupancy (left) and signal strength of GPS observations tracked by S-3A on 2022/09/01.

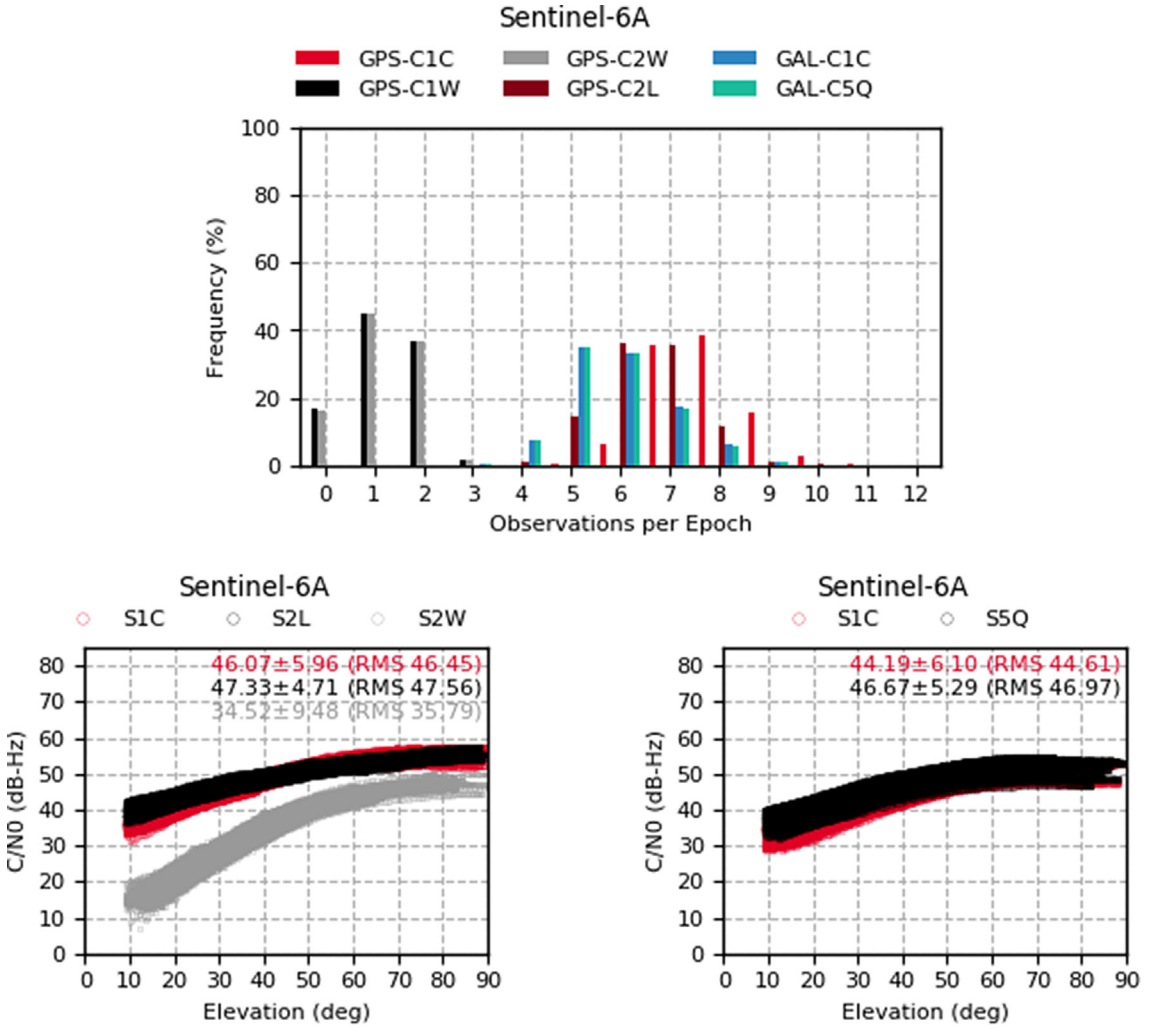

Fig. 7. Channel occupancy of GNSS observations (top) and signal strength of GPS (bottom left) and Galileo (bottom right) observations tracked by S-6A on 2022/09/01.

3. Description of the CPOD Service

The CPOD Service provides operationally precise orbit products and other auxiliary data files and provides them on time to the corresponding PDGS / PDAP to support the product generation of the Copernicus services. Examples of applications that need POD include SAR, Interferometric SAR, and altimetry.

GMV, a Spanish company with a large experience in POD and GNSS, was granted an initial contract by ESA to develop the CPOD Service, back in 2013. The initial industrial consortium led by GMV included POSITIM, DLR and TUM. In 2015, the consortium was enlarged with AIUB and TUD. In parallel, the UK company VERIPOS was granted a contract in 2014 to provide the GPS orbits and clocks necessary to carry out the POD in NRT and STC. For NTC products the IGS (International GNSS Service, Johnston et al., 2017) final products were used originally. In 2020, a second contract was granted to the GMV´s consortium, with a couple of modifications: VERIPOS was substituted with GMV´s ***magicGNSS*** products, and GFZ was included in the consortium. Finally, in 2022, a third contract was granted to GMV´s consortium for another 5 years.

The CPOD Service generates orbit products and auxiliary files as summarized in Table 3. The format of the products and files is described in (Fernández, 2022).

The CPOD Service generates precise orbit products, of different timeliness and accuracies, for the four Copernicus Sentinel missions mentioned. The **predicted orbits** (PRE) of Sentinel-1 are generated as soon as new GNSS L0 data is available. They have a coverage of four orbits starting at the last ascending node available with GNSS data. Therefore, this product has a small restituted interval and the rest is a propagation. The accuracy requirement is only applicable to the first orbit within the product. This product was available from Q4 2019 onwards to be used instead of the on-board navigation solution.

The **restituted orbits** of all missions are generated as soon as new GNSS L0 data files is available. The coverage of the products is different per mission, but typically includes between 1 and 3 orbits backwards from the last GNSS data available. The **medium and precise orbits** are computed at fixed latencies associated to the requirements. They are typically better than the restituted orbits because the quality of the auxiliary products used (particularly the GNSS orbits and clocks) is better.

The auxiliary files include **platform data files**, that contain information about the misalignment of the platform with respect to the theoretical attitude. Currently, these are only generated for Sentinel-3.

Then, **GNSS L1b RINEX and quaternions** files are generated from the decoding of the GNSS and quaternions L0 data downloaded from the satellite. While the quaternions are just a simple conversion from binary to ASCII, the generation of RINEX files needs some processing, to define a time scale. There are three possibilities: the i) GNSS on-board time scale, the Instrument Measurement Time (IMT), ii) the GPS/GNSS time, and iii) a polynomial fit to the GPS/GNSS time. Additionally, the GNSS observations can be calibrated to remove constant and temperature dependant biases.

Finally, the **CPF file** is an orbit prediction used by the ILRS stations to track satellites with laser. In this case, the CPOD Service just generates the CPF for the Sentinel-3 mission, while EUMETSAT generates the corresponding file for Sentinel-6 MF.

The CPOD Service also makes available other information to users, including manoeuvre information, the evolution of the mass and centre of mass coordinates of the satellite, the GNSS data gaps, and the in-flight generated GPS/GNSS antenna calibrations.

This section describes firstly the physical design of the CPOD Service, followed by a description of the logical design corresponding to the SW components and processing logic that implements the business logic of the CPOD Service. This is presented through the following areas (Fig. 8):

- **Interfaces**: the external data and products used to compute the precise orbits (section 3.2)
- **Storage and dissemination**: how the data and products are obtained, disseminated, and archived in the CPOD system (section 3.3).
- **Data & process management**: how the CPOD Service is orchestrated to generate the products (section 3.4).

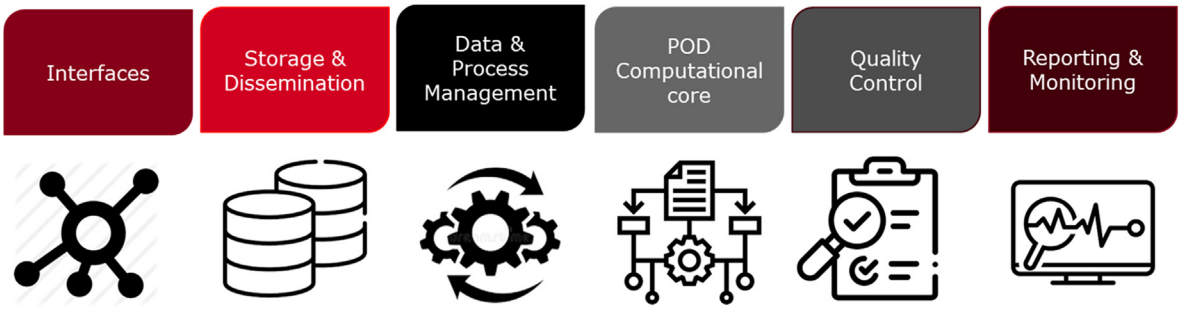

Fig. 8. Elements of the logical design of the CPOD Service.

- **POD computational core**: the POD software (section 3.5).
- **Quality control**: the approach used to monitor the quality of the products (section 3.6).
- **Reporting and monitoring**: the tools used to report the status of the CPOD Service and the quality of products (section 3.7).

3.1. Physical design

The physical design of the CPOD Service was done considering the demanding requirements asking for the delivery of at least 99.5 % of the products, with the required accuracy and timeliness, and that the system cannot be down more than 24 h. Therefore, the system is designed to have two levels of **redundancy**.

The first level is on the **interface** with the clients, to receive the inputs and deliver the products. The system exposes a unique IP, which is internally mounted as a high-availability system composed of two machines (master and slave). Both machines support different communication protocols (FTP, FTPS, SFTP, HTTPS) and have a shared disk to keep the input/output data.

The second level of redundancy is on the **processing** side. Considering the time available for the NRT products (currently below 10 min since the availability of the GNSS data), there is no time for manual intervention. Therefore, the system is designed to have two independent processing machines running in parallel, processing the same inputs. The processing on one of the machines is delayed by few minutes to avoid colliding when publishing the product, but still fulfilling the requirements. Each processing machine has its own archive and databases (DBs), so they are completely autonomous from each other.

In addition to the interface and processing machines, the CPOD Service is complemented with Firewalls, monitoring and validation machines, and an FTP server used to share information with the CPOD QWG and the ILRS.

Until mid-2019, the physical elements of the CPOD Service were running on the GMV´s premises in Tres Cantos, Madrid (Spain). After this, it was moved to a **public Cloud** hosted by the company GIGAS, also in Madrid. Currently, the physical design is composed of 10 machines, 80 CPU cores, 120 GB of RAM, 1.2 TB of hard disk memory and 10 TB of archive.

This design allows supporting the four Sentinel missions, with a total of seven satellites. Overall, the CPOD Service generates approximately 100,000 orbit products per year.

3.2. Interfaces

This section summarizes the inputs and products used and generated by the CPOD Service.

- **GNSS & NAVATT L0**. Each satellite is equipped with a GPS/GNSS receiver that generates raw (binary) data including i) measurements (pseudo-range, carrier phase, Doppler and CN0), ii) the on-board navigation solution computed by the GNSS receiver (position and velocity as a function of time), and iii) the GNSS navigation message tracked by the GNSS receiver.
  Additionally, each satellite is also equipped with star trackers to support the attitude control of the satellite. They generate **quaternions**, at 1 Hz, that are also downlinked as binary data.
  The rate of the GNSS measurements depends on the mission (Table 4): the receivers on-board Sentinel-1 A&B and Sentinel-2 A&B generate them every 10 s, but the observations are not at the multiple of ten seconds. The counting is initiated when the receiver starts its tracking. For Sentinel-3 and −6 the observables are generated every second; for Sentinel-6 MF the pseudo-range is only transmitted on seconds multiple of 10 to save bandwidth when downloading data from the satellite.
- **Flight Dynamics products**. These products include the manoeuvre information (i.e., the manoeuvre start and stop times and accelerations per orbital axis), the evolution of the mass and centre of mass change after each manoeuvre, and the restituted and predicted orbits computed by Flight Dynamics, using typically ranging from ground and the on-board navigation solution computed by the GPS/GNSS receiver. The FOS for Sentinel-1 and −2 is ESOC, while for Sentinel-3 and −6 it is EUMETSAT.
  The manoeuvre information is typically planned and delivered one week in advance, except when a collision avoidance manoeuvre (CAM) is required; in this case, the manoeuvre information can be generated few hours before. The CPOD Service needs to check and update this information quickly, to avoid impacting the accuracy of the orbit products.
- **GNSS products**. The CPOD Service computes the precise orbits of the Sentinels using GNSS observations. This requires a precise knowledge of the GNSS orbits,

Table 4
Rate of GNSS measurements per mission.

Measurement	Sentinel-1 A&B	Sentinel-2 A&B	Sentinel-3 A&B	Sentinel-6 MF
Pseudo-range	10 sec (1)	10 sec (1)	1 sec	10 sec (2)
Carrier-phase	10 sec (1)	10 sec (1)	1 sec	1 sec

(1) Not multiple of 10
(2) Multiple of 10

Table 5
EGP / CODE products used by CPOD Service.

GNSS Product	Coverage	Frequency of products	Frequency of data	Format
15 M orbits & clocks	30 min	15 min	30 s	SP3[12]
24H orbits	2 days	Hourly	15 min	SP3
24H clocks	1 day	Hourly	30 s	Clock RINEX[13]
STC orbits	1 day	Daily	15 min	SP3
STC clocks	1 day	Daily	30 s	Clock RINEX
CODE orbits	1 day	Weekly	5 min	SP3
CODE clocks	1 day	Weekly	5 s	Clock RINEX
CODE biases	1 day	Weekly	n/a	SINEX Bias[14]

[12] https://files.igs.org/pub/data/format/sp3c.txt.
[13] https://files.igs.org/pub/data/format/rinex_clock304.txt.
[14] https://files.igs.org/pub/data/format/sinex_bias_100.pdf.

clocks, and biases. Here, there are two requirements that are somehow contradictory. GNSS products are required with short timeliness, as they are needed by the NRT processing firstly. However, the longer the latency to generate the GNSS products is, the better accuracy can be achieved. Therefore, the CPOD Service designed a scheme to fulfil all requirements using different inputs (Table 5):

- For the NRT processing, the EGP provides GNSS orbits and clocks every 15 min, with a coverage of 15/30 min. Additionally, the EGP generates products every hour, with a coverage of 24 h. Until October 2020, these products were generated by VERIPOS (UK), with the back-up of GMV´s ***magicGNSS*** service. After that, ***magicGNSS*** provides them, with the back-up of DLR´s RETICLE service until December 2022, when DLR´s RETICLE was discontinued. Currently, it is only ***magicGNSS*** which provides these products.
- For the STC processing, the EGP generates daily products, with 24 h of coverage, with a slightly better accuracy as those computed in NRT.
- For the NTC processing, the GNSS products are obtained from IGS and CODE (Center for Orbit Determination in Europe, Dach et al. 2020a,b). Until May 2020, the CPOD NTC´s processing was not using IAR, and therefore, it was not necessary to use GNSS phase biases. Additionally, until November 2020, all satellites were tracking GPS only, and therefore, there was no need of Galileo products. Therefore, until May 2020, IGS final products were used for the NTC processing. After that, CODE products are used to make use of the GPS + Galileo products, and their biases to apply IAR. As a back-up, if they are not available, the computation is based on the IGS products.

Fig. 9 shows an overview of the external interfaces of the CPOD Service.

– **Geodynamic products**. This includes the Earth Orientation Parameters (EOPs) and Leap Seconds, the Solar Activity indexes, the Atmospheric and Ocean Dealiasing product and in the near future, the COST-G geopotentials.

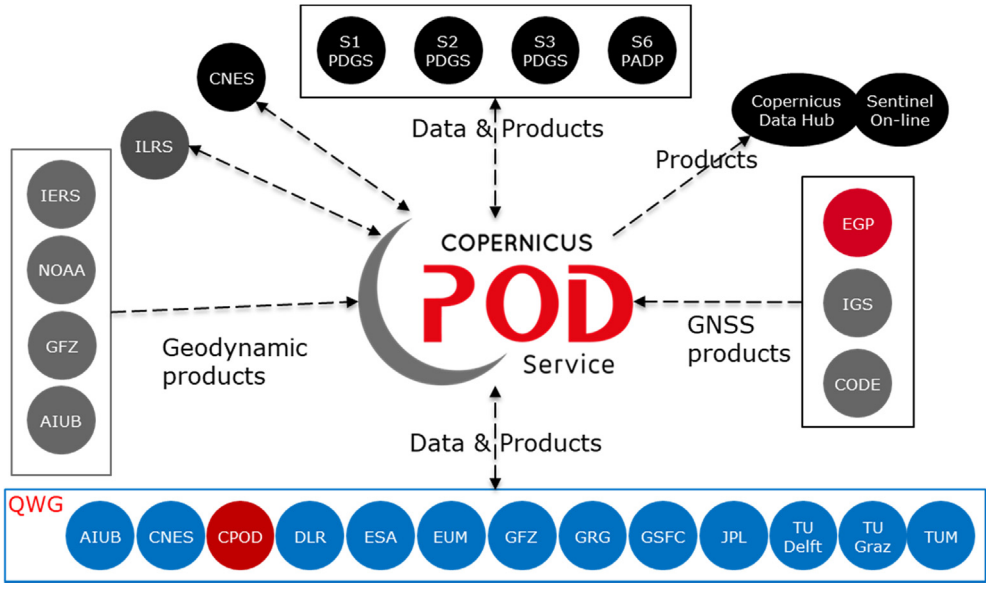

Fig. 9. Overview of external interfaces.

Table 6
Summary of operational orbit products generated by CPOD Service.

Mission	NRT	STC	NTC
Sentinel-1	Predicted Restituted	n/a	Restituted
Sentinel-2	Predicted (1) (2) Restituted (1)	n/a	Restituted
Sentinel-3	Restituted	Predicted (ILRS) (1) Restituted	Restituted
Sentinel-6	Restituted	n/a	n/a

(1) Not available in CDSE
(2) Until December 2022

– **DORIS & SLR observations**. The Sentinel-3 and −6 missions are equipped with a DORIS and a LRR instrument. CNES generates DORIS RINEX data, while ILRS provides SLR observations from the stations tracking Sentinel-3 and −6.
– **External orbit products**. The CPOD Service receives precise orbits from three external centres: i) daily from CNES for Sentinel-3 A&B and Sentinel-6 MF, ii) daily from ESOC (until 2021), and TUD (2021 onwards) for all Sentinels, and iii) quarterly from CPOD QWG for all Sentinels (section 3.6.2.1).

The CPOD generates the following types of products:

- **Operational orbit products** (Table 6) for the respective PDGS/PDAP in an Earth Observation File (EOF) in XML format (Fernández, 2022). There are different products associated to different latencies (NRT, STC, NTC) and purposes (predicted and restituted). Besides the products for the PDGS/PDAP, the CPOD Service also generates CPF files of Sentinel-3 to support SLR tracking.
  Most of these products are also available to external users, through the CDSE. This is a web-based interface that the Copernicus program exposes to all external users, to provide complete, free, and open access to data and products.
- **Platform data files** for the Sentinel-3 mission. These products include the deviation of the platform with respect to the nominal (modelled) attitude. They are generated in NRT, STC and NTC timeliness. The format is XML. These products are also available to external users through the CDSE.
- **GNSS RINEX** for Sentinel-3 and −6 mission. Hourly and daily GNSS L1b RINEX files are generated for CNES (S-3 and S-6) and JPL (Jet Propulsion Laboratory) (S-6). These RINEX files have the particularity that the epochs of the measurements follow the IMT. This causes that the epochs diverge with respect to the GPS time scale; it is realigned when the difference reaches 10 ms.
- **GNSS RINEX files & Quaternions** for external users. Daily files are generated and published on the CDSE. The GNSS RINEX files are generated with a different strategy: for S-1 and S-2, the epochs are aligned to the GPS time estimated on-board. For S-3 and S-6, the epochs are aligned to a polynomial fit to GPS time. This second approach can be used only when the stability of the clock is good enough, which is the case for S-3 and S-6 thanks to the use of an USO.
  The quaternions are computed on-board by the star tracker, but they are processed by the CPOD Service to interpolate them to the integer GPS second, and to fill gaps with the nominal attitude of the corresponding satellite.
- **Others**: The CPOD Service provides other auxiliary information to external users through the Sentinels Online.[15] The Sentinel Online is a web-based portal to provide information about the Sentinel missions to all external users. The CPOD Service provides routinely the manoeuvre information, the mass and centre of mass evolution and the Phase Centre Offset and Variations (PCO/PCV) of the GNSS antennas on-board the Sentinels.

3.3. Storage and dissemination

The CPOD Service has been storing all the inputs received and products generated since the beginning of the service in 2014. Currently it archives more than 3.5 TB of data and products. Additionally, all processing and QC metrics are stored in DBs allowing an easy access for reporting and monitoring (see section 3.7).

From the point of view of the external users (i.e., PDGS/PDAP and CNES), there are two mechanisms that are used to get & put inputs and products: secure FTPs and secure servers using HTTPS API REST protocols.

3.4. Data & process management

The data and process management currently used by the CPOD Service is based on an **orchestration**, understood as

[15] https://sentinels.copernicus.eu/web/sentinel/home.

having a scheduler (Linux crontab) that triggers the execution of the processes. There are two types of processing:

- Those that have demanding timeliness requirements. This includes the generation of all NRT orbit and platform products, and the hourly RINEX files. They are launched every minute to check if new input data is available. It also includes the checking for input data, which is done every minute.
- Those that have relaxed timeliness requirements. This includes the generation of STC and NTC orbit and platform products and the quality control. They are launched at a specific time, once or few times per day.

3.5. POD computation core

The POD computation core is composed by the SW in charge of:

- **Decoding** the input L0 GNSS & NAVATT packages into ASCII files.
- Performing the **POD** and generating the products. This is the most complex part of the SW, which is described below.
- Performing the **Quality Control**, which is described in section 3.6.

Currently, these different tasks are carried out by several SW programs, which can be divided into:

- **L0 decoders**: this SW is written in C++. It generates ASCII files with the GNSS observations (RINEX observation), navigation solution (SP3), GNSS BRDC (RINEX navigation) and quaternions.
- **NAPEOS**: This is an ESA/ESOC, state-of-the-art POD SW package, written in Fortran 90/95 and TCL/TK. It is composed by numerous programs, each of them in charge of a specific task like input preparation, measurements pre-processing, POD, product formatting, comparisons, etc.

GMV has been developing a new POD SW called ***focusPOD*** (Fernández et al., 2023), which has substituted the L0 decoders and NAPEOS from end of January 2023 onwards. Written in C++ and Python from scratch, it has been designed as a multi-purpose library, from which it is possible to build ad-hoc or generic programs.

The generation of precise orbits is split into the following steps:

- **Retrieval of inputs**: All inputs are retrieved from external sources and archived into the CPOD Service by independent chains. Therefore, this step just consists in selecting the best inputs (L0 GNSS & NAVATT, GNSS products, geodynamic inputs, FOS inputs, etc.) querying to the CPOD DB.
- **L0 decoding**: The GNSS & NAVATT L0 binary data is decoded to obtain the GNSS observations, the on-board navigation solution, and quaternions.
- **GNSS products handling**: The EGP provides GNSS products with different coverages and timeliness. This task generates consolidated GNSS orbit and clock products with the coverage that fits the determination interval used. Typically, this requires merging the content of several input files.
- **GNSS Pre-processing**: The raw GNSS observations are combined to generate ionosphere-free linear combinations. Then, several checks are performed to identify and reject outliers. Afterwards, passes are identified, and an initial ambiguity is computed. Finally, using the ionosphere-free pseudo-range observables with the Bancroft algorithm (Bancroft, 1985), an initial Position, Velocity & Time (PVT) of the LEO satellite is computed as a rough initial solution.
- **Least Squares Adjustment**: The POD problem is parametrized as a reduced-dynamic problem solved with Least Squares Adjustment, in which several parameters are estimated per determination arc: initial state-vector, drag (CD) and solar radiation (RP) coefficients, Constant-per-revolution (CPR) empirical accelerations, manoeuvre calibrations, clock biases and float ambiguities per pass. Table 7 lists the current parametrization.
- **IAR**: In this step, the float ambiguities are fixed using the method described in Montenbruck et al. (2018). This step is done currently only for the NTC products, as it requires the code and phase GNSS biases. It is planned to apply IAR for the STC and NRT timeliness, once the ***magicGNSS*** delivers biases in the future. After fixing the ambiguities, the POD Least Square adjustment is done once more to compute the final precise orbit.
- **Product generation**: The final product is formatted into EOF, CPF or SP3, as required.
- **Archive**: The final product is archived in the CPOD Service prior to its dissemination. Additionally, processing metrics are dumped into the DB.
- **Dissemination**: New products are disseminated to their final user, which can be the PDGS/PDAP or the CDSE.

3.5.1. Evolution of POD algorithms, software, and inputs of CPOD Service

Since 2014, the CPOD Service has experienced significant evolutions in the software, algorithms, and inputs used. The main changes are listed in Table 8. The following changes are considered as major evolutions:

3.5.1.1. Integer ambiguity resolution. The use of single receiver, integer ambiguity resolution algorithms was introduced in May 2020. This algorithm is only used in NTC and for reprocessing, as it requires GNSS code and phase biases. The CPOD Service is using the products from CODE, but they are available with a latency that prevent its use in NRT or STC.

Table 7
POD Parametrization (as of end of 2022).

Parameter / Model	Value
Software	
Name and version	NAPEOS
Arc Cut	
Arc lengths	NRT: 24 h STC/NTC: 32 h
Handling of manoeuvres	Manoeuvres are calibrated in the POD process
Handling of data gaps	Yes
Reference System	
Polar motion and UT1	IERS finals2000A.data (Petit and Luzum, 2010)
Pole model	IERS 2010 Conventions (Petit and Luzum, 2010)
Precession/Nutation	IERS 2010 Conventions
Satellite Reference	
Mass and centre of gravity	Variable with input from FOS
Attitude model	Quaternions
GNSS antenna reference point and orientation	Fixed as per configuration
Gravity	
Gravity field (static)	EIGEN.GRGS.RL04 TVG (120x120) (Lemoine et al., 2019)
Gravity field (time varying)	Drift/annual/semi-annual piece-wise linear terms up to degree/order 90 (Lemoine et al., 2019)
Solid Earth tides	Applied (IERS 2010)
Ocean tides	FES2014 (100x100, 142 tidal constituents) (Lyard et al., 2021)
Atmospheric gravity	GFZ AOD L1B RL06 (100x100) (Dobslaw et al., 2017)
Atmospheric tides	GFZ AOD L1B RL06 (100x100)
Earth pole tide	IERS 2010
Ocean pole tide	IERS 2010
Third bodies	Sun, Moon, Planets DE-421 (Folkner et al., 2009)
Surface Forces and Empiricals	
Radiation pressure model	Macro model (with re-radiation)
Earth radiation	Albedo and infrared applied
Total Solar Irradiance (TSI)	n/a
Atmospheric density model	msise00 (Picone et al., 2002)
Radiation pressure coefficient	Fixed 1 coefficient to 1.0
Drag coefficients	Estimated 1 coefficient per arc (constrained with 0.3)
1/rev empirical accelerations	Estimated every 12 h for NRT and every 2 h for STC/NTC in the along and cross-track directions, the following components: - constant (constrained to 10^{-12} km/s^2) - sine and cosine (constrained to 10^{-11} km/s^2)
GNSS Measurements	
Relativity	Applied (IERS 2010)
Sampling	10 s
Observations	Ionosphere-free linear combinations of phase and pseudo-range measurements
Weight	0.8 m (pseudo-range) / 10 mm (carrier-phase)
Elevation angle cut-off	7 deg
Down-weighting law	None
Antenna phase-centre wind-up correction	Applied
Antenna phase-centre variation	Applied (sen08_2170.atx)
GNSS Parameters	
Receiver clocks	Per epoch, every 10 s
Receiver ambiguities	Estimated (integer)
GNSS orbits	Fixed; CODE final (Dach et al. 2020a), CODE rapid (Dach et al., 2020b) for S6A
GNSS clocks	Fixed (CODE final, 5 s, CODE rapid for S6A)
GNSS satellite biases	CODE finals

Table 8
Processing evolutions in the CPOD Service.

Parameter	v0.8.4	v0.8.7	v1.2.0	v1.5.5	v1.6.0	v1.10.0	v2.0.0	v3.0.0
Date	Sep 2014	Jan 2015	Dec 2016	Oct 2019	May 2020	Feb 2021	Nov 2022	Jan 2023
POD SW	NAPEOS							***FocusPOD***
IERS Conventions	IERS 2003 (McCarthy and Petit, 2004)	IERS 2010 (Petit and Luzum, 2010)						
Gravity Field	EIGEN-GL04C (Förste et al., 2006)	EIGEN6S (Rudenko et al., 2014)	EIGEN.GRGS.RL03.v2 (Lemoine et al., 2015)		EIGEN.GRGS.RL04 TVG (120x120) (Lemoine et al., 2019)			
Ocean Tides	FES2004 (Lyard et al., 2006)	EOT11a (Savcenko et al., 2012)			FES2014 (100x100, 142 tidal constituents) (Lyard et al., 2021)			
Atmospheric gravity	AGRA (https://massloading.net)				GFZ AOD L1B RL06 (100x100) (Dobslaw et al., 2017)			
Number of drag parameters	6/24 h					NRT: 10/24 h STC/NTC: 1		
Solar radiation pressure	1 estimated					NRT: 1 estimated STC/NTC: 1 Fixed		
Empirical accelerations	2/24 h Sine/Cosine in Along/Cross			NRT: 2/24 h STC/NTC: 3/32 h Sine/Cosine in Along/Cross		NRT: 2/24 h; Sine/Cosine in Along/Cross STC/NTC: 16/32 h; Constant/Sine/Cosine in Along/Cross		
Phase ambiguity	Float					NRT/STC: Float NTC: Integer		
ITRF	IGb08 (Rebischung, 2012)				IGS14 (Rebischung and Schmid, 2016)		IGS20 (Villiger, 2022)	
GNSS products	NRT/STC: EGP NTC: IGS finals					NRT/STC: EGP NTC: CODE rapid/finals		

3.5.1.2. Orbit modelling. A reduced-dynamic orbit modelling was already used from the beginning of the service operations, but it was not until February 2021 that a more reduced-dynamic orbit parametrization was included. The empirical accelerations changed from 2 sets per 24 h to 16 sets for the STC and NTC processing. For NRT, the number of empirical parameters is still 2, as it has a significant impact on the time to solve the problem, which is critical for the NRT processing.

3.6. CPOD quality control

The CPOD Service includes several Quality Control activities to assess the quality of the operational products generated in order to ensure their correctness and accuracy. They are divided into **Routine Monitoring** and the **Regular Service Reviews**.

3.6.1. Routine monitoring

The routine monitoring encompasses the automatic tasks done by the CPOD Service system, to evaluate POD processing metrics and rapid orbit comparisons that allow to identify degraded products and to monitor the behaviour and quality of inputs and products. These tasks can be subdivided in two areas:

- **Monitoring POD processing metrics**. The POD processing generates numerous metrics which are related directly or indirectly with the quality of the products. This includes the number of GNSS satellites in view, the number of used and rejected GNSS observations, the GNSS pseudo-range and carrier-phase root mean square (RMS) residuals, SLR residuals, the percentage of fixed ambiguities, the presence of manoeuvres or data gaps, the estimated parameters (particularly the drag and solar radiation pressure scale factors, empirical accelerations, and manoeuvres), etc. All these metrics are available upon generation of each product. They are dumped into a DB for online monitoring and used to flag the generated products with a quality flag (indeed, each state-vector in the product).
- **Rapid orbit comparisons**. The direct orbit comparison with an independent solution is the other routine method used, together with the calculation of overlap comparisons between consecutive products. The CPOD Service has been receiving independent orbit solutions of all Sentinels, with a latency of 1 day, from ESOC until 2021 and since beginning of 2022 from TU Delft. In addition, CNES is computing operational orbits of Sentinel-3A & B, and Sentinel-6 MF, which are also used for comparisons.

These two methods are used by the POD operators to monitor quickly that the accuracy requirements are maintained, to identify and correct issues in the processing and to quickly warn the final users of potential degradations in the quality of products.

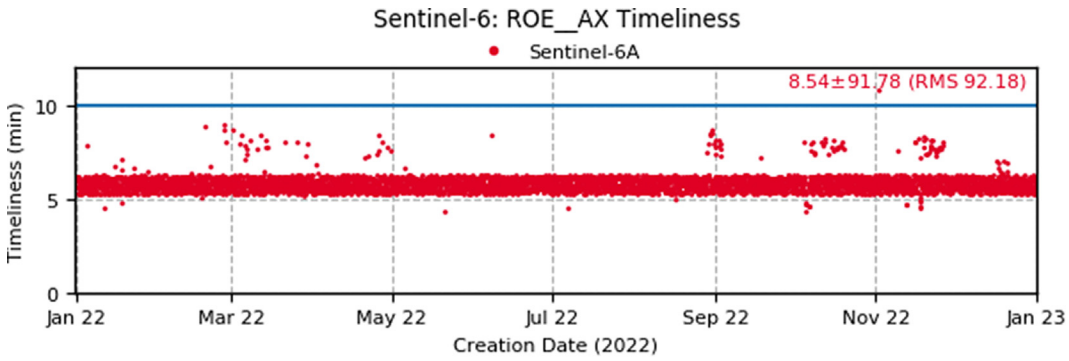

Fig. 10. Timeliness of the generation of Sentinel-6 MF NRT orbit products (year 2022).

3.6.2. Regular service review

While the routine monitoring can be done during the nominal operations, the RSR is done a-posteriori, with a frequency of 3 to 4 times per year, covering the previous period. This is a thorough analysis that requires the support of the CPOD QWG (see section 3.6.2.1). The activities involved in the RSR are detailed hereafter.

Analysis of timeliness and availability: it consists of the analysis of the number and timeliness of inputs received (including EGP inputs) and products disseminated. The results are interpreted and traced down to those anomalies that occurred during the reporting period. Fig. 10 shows the remarkable timeliness of the NRT generation of Sentinel-6A, from the availability of the input GNSS data, to the dissemination of the product.

Generation of the combined orbit solution: Using the independent orbit products generated by the CPOD QWG (see Table 9), the CPOD Service generates a combined orbit solution as a weighted mean of them. The method firstly generates an orbit as an unweighted mean of the orbits participating in the combination. Then, each of the orbits participating in it, are compared against the unweighted mean, from which the final daily weights are derived. The final step is to generate the new orbits as a weighted mean. This approach is done several times to identify outliers that can jeopardize the quality of the products. Kobel et al. (2019) propose and compare a different algorithm for orbit combination using Variance Component Estimation.

Comparison of orbit solutions against combined orbits: The combined solution is then used to compare all operational products against it. Additionally, the orbit solutions provided by the CPOD QWG centres are also compared against the combined solution. From these comparisons, the 3D and radial RMS is computed per product. Fig. 11 shows for instance the radial RMS of the comparison of Sentinel-6 MF ROE products and the combined solution, over year 2022. Each dot corresponds to a product which covers one orbit. Vertical red lines indicate manoeuvres, and the blue horizonal line is the requirement.

Fig. 12 shows the daily radial RMS of the comparisons of Sentinel-6 MF daily orbits generated by the CPOD QWG

Table 9
List of CPOD QWG members providing orbit products.

Institution	POD SW	Strategy	Tracking	Missions	CPOD Consortium (2023 –)	Crossover analysis
AIUB	Bernese v5.3 (Dach et al., 2015)	Kinematic & Reduced dynamic	GNSS	ALL	NO	NO
CLS	GINS/DYNAMO (CNES/CLS 2023)	Reduced dynamic	DORIS	S-3, S-6	NO	NO
CNES	ZOOM v6.0 (Carrou, 1986)	Reduced dynamic	GNSS + DORIS	S-3, S-6	NO	NO
DLR	GHOST v2276 (Wermuth et al., 2010)	Reduced dynamic	GNSS	ALL	YES	NO
ESOC	NAPEOS v4.7 (Springer et al., 2011)	Reduced dynamic	GNSS	ALL	NO	NO
EUMETSAT	NAPEOS	Reduced dynamic	GNSS	S-3, S-6	NO	NO
GFZ	EPOS-OC v6.74 (Rudenko et al., 2011)	Reduced dynamic	GNSS	ALL	YES	NO
GMV	NAPEOS (- 2022) ***FocusPOD*** *(2023 -)* (Fernández et al., 2023)	Kinematic & Reduced dynamic	GNSS	ALL	YES	NO
GSFC	GEODYN (NASA 2023a)	Reduced dynamic	DORIS + SLR	S-6	NO	NO
JPL	GIPSY-OASIS v6.4 (NASA 2023b)	Reduced dynamic	GNSS	S-3, S-6	NO	NO
TUD	GIPSY-X v1.7 (Bertiger et al., 2020)	Reduced dynamic	GNSS	ALL	YES	YES
TUG	GROOPS (Mayer-Gürr et al., 2021)	Reduced dynamic	GNSS	ALL	NO	NO
TUM	Bernese v5.3	Reduced dynamic	GNSS	ALL	YES	YES

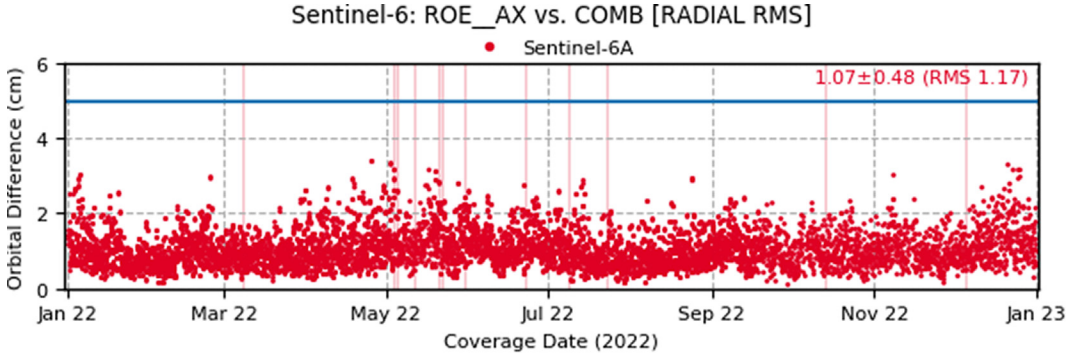

Fig. 11. Sentinel-6 MF NRT products vs. Combined orbit [Radial RMS; cm] (the accuracy requirement is shown with a blue line).

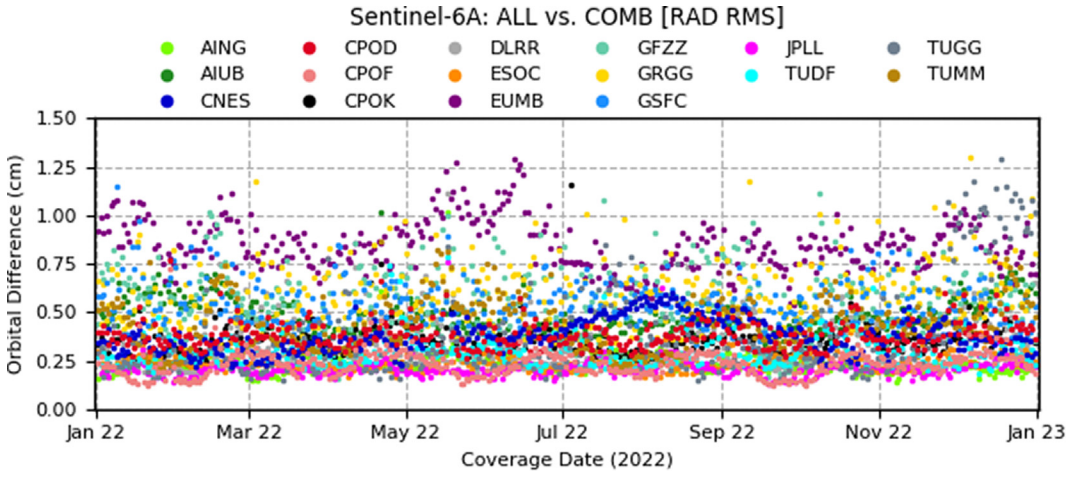

Fig. 12. Sentinel-6 MF orbit comparisons – CPOD QWG solutions vs. COMB [radial RMS; cm].

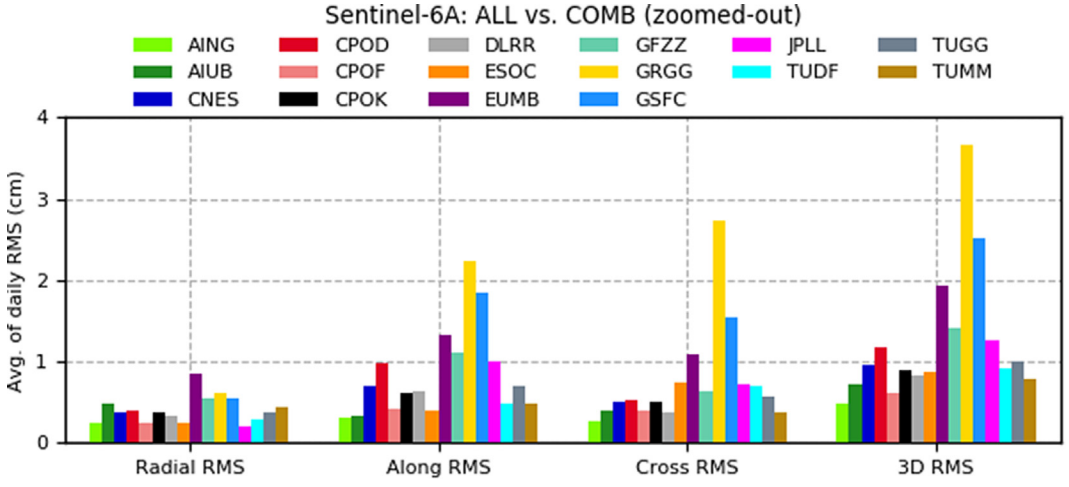

Fig. 13. Sentinel-6 MF orbit comparisons – CPOD QWG solutions vs. COMB [average of daily RMS per component; cm].

and the combined solution, over year 2022. Each dot corresponds to a daily product. Fig. 13 shows the average of daily RMS per component and centre, while Fig. 14 shows the average of daily mean per component and centre.

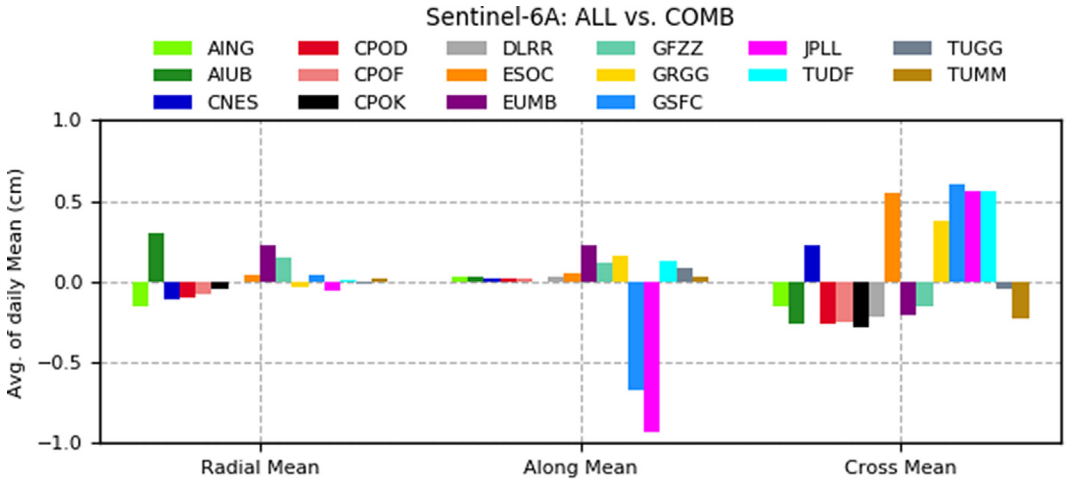

Fig. 14. Sentinel-6 MF orbit comparisons – CPOD QWG solutions vs. COMB [average of daily mean per component; cm].

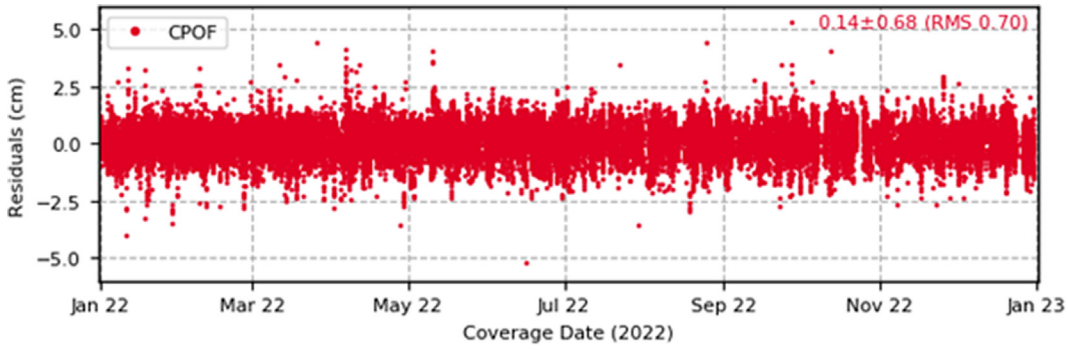

Fig. 15. Example of SLR residuals of Sentinel-3B (year 2022).

Generation of GNSS Sensor Performance Report: The performance of the GNSS receiver is evaluated through several metrics:

- Distribution of observables per azimuth and elevation in the receiver antenna frame
- Histogram of number of observations per epoch and signal
- Daily average of number of GNSS observations
- GNSS Signal Strength as function of elevation
- Evolution of dilution of precision (DOP) as a function of time
- Analysis of the stability of the USO on-board S-3 and S-6

Evaluation of SLR residuals for S-3 and S-6: The SLR data can be used in POD as additional observables, or just to estimate the SLR observation residuals without considering them in the orbit determination, which is the approach used by the CPOD Service. This method provides an independent method to derive the accuracy of the orbit products, at least in the radial direction (which is the relevant direction for the S-3 and S-6 altimetry missions). The procedure used by the CPOD Service includes firstly the estimation of a range bias per station and satellite over a period of 4 weeks using the combined solution. Then the SLR residuals are calculated after removing the calculated station range biases. The final outcome are a series of plots and statistics that validate the accuracy of the different NTC orbits solutions, including the solutions provided by the CPOD QWG (see example in Fig. 15).

Evaluation of altimetry cross-over analysis for S-3 and S-6: Altimetry crossovers (i.e., altimeter measurements taken at crossing ground-tracks from two different passes, which can belong to the same or to different satellites) are typically used to extract information about the sea surface height variations on a given geographical location. The differences in altimeter measurements at crossovers are impacted by radial orbit variations, sea surface variability over time, altimeter noise and altimeter calibrated biases. Therefore, assuming that the altimetry processing is good enough and that the ocean signals are properly considered, altimetry cross-over residuals can be considered to reflect radial errors in the orbit solutions. This analysis is done by TUD and DGFI-TUM (Bosch and Savcenko, 2007; Bosch et al., 2014). Examples of these analysis can be found on the yearly service reviews of 2021 and 2022 under Sentinel Online.

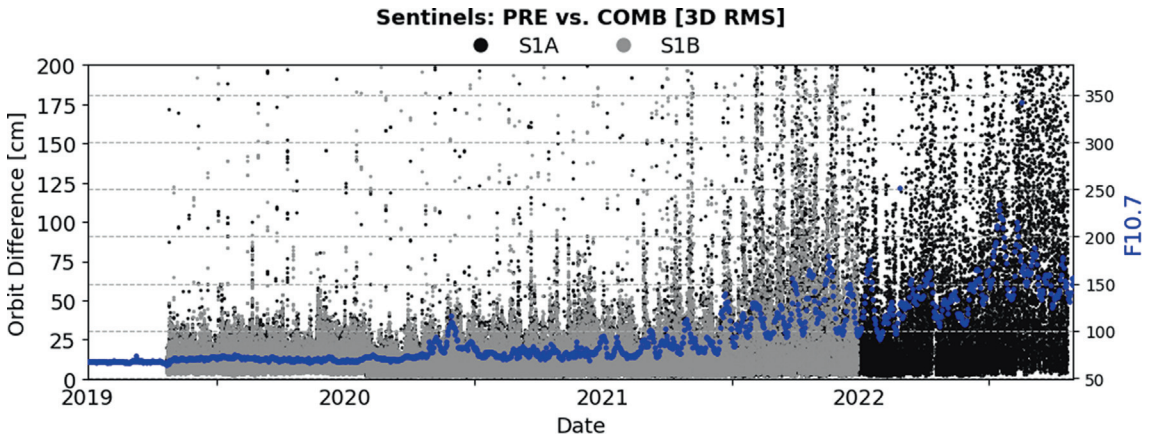

Fig. 16. Orbital accuracy of Sentinel-1 predicted vs. combined products [3D RMS over one orbit].

Analysis of EGP performance: the accuracy of the GNSS orbit and clock products generated by the EGP is analysed, comparing them against the CODE rapid products.

These analyses are documented and published on the Sentinel Online.[16]

3.6.2.1. CPOD quality working group. The main purpose of the CPOD QWG is to monitor the performance of the operational POD products (both the orbit products as well as the input tracking data) of the Sentinel-1, −2, −3 and −6 missions, and to define potential and future enhancements to the orbit solutions. As part of this role, several members of the CPOD QWG (Table 9) provide independent orbit products which are combined to generate a reference, combined orbit, which is then used to assess the quality of the operational products. Additionally, once per year, two institutions (TU Delft and TU Munich) perform a Satellite Altimetry Cross-Over analysis of the Sentinel-3 & −6 orbits.

3.7. Reporting & monitoring

The following two tools support the monitoring of the CPOD System:

- **NAGIOS** is used to monitor the machines, networks, availability of inputs and products, and the nominal functioning of the system. A 24x7 service identifies issues with the machines and networks, and contact the Cloud provider in case of problems.
- **Grafana** is used for the online monitoring. The POD experts use this tool to monitor not only the availability of inputs and products, but also the timeliness, and quality control metrics which are generated routinely.

[16] https://sentinels.copernicus.eu/web/sentinel/technical-guides/sentinel-3-altimetry/pod/documentation

4. Results and discussion

This section presents, in subsection 4.1, the accuracy obtained by the different operational products, since the beginning of the CPOD Service in 2014. As such, it visualizes the major modifications in the configuration of the POD, including the update of the models. Subsections 4.2 and 4.3 focus on the sub-daily accuracy of the most accurate products of Sentinel-1A and −3A, as an example of the current state-of- the-art.

Here, accuracy is measured by comparing against a combined orbit solution, computed as described in section 3.6.2, considering between 7 and 11 independent orbit solutions. For Sentinel-3 and −6, the use of SLR residual analysis is also considered, as an independent accuracy metric.

4.1. Overview

4.1.1. Predicted orbits

The Sentinel-1 mission required originally only NRT and NTC products, but at the end of 2019, after an extensive validation, a new predicted orbit product was included to substitute the use of the on-board navigation solution (NAV) in the most rapid production service, which is launched just after the download of new SAR data from the satellite. The predicted product contains four orbits, starting from the last ascending node included in the available GNSS data used for the orbit determination. In terms of quality control, only the first orbit is considered, that includes a small, determined interval, and the rest is predicted.

Fig. 16 shows the 3D RMS of the differences between the first orbit within the predicted product and the combined solution; superimposed is also the daily solar activity index F10.7 to highlight the relationship between both metrics. Fig. 17 shows the yearly 1-sigma of the 3D RMS (per product) showing visually the effect of the increasing solar activity. In the years from 2019 to 2021, the 1-sigma was below 15 cm. but increases afterwards up to more than

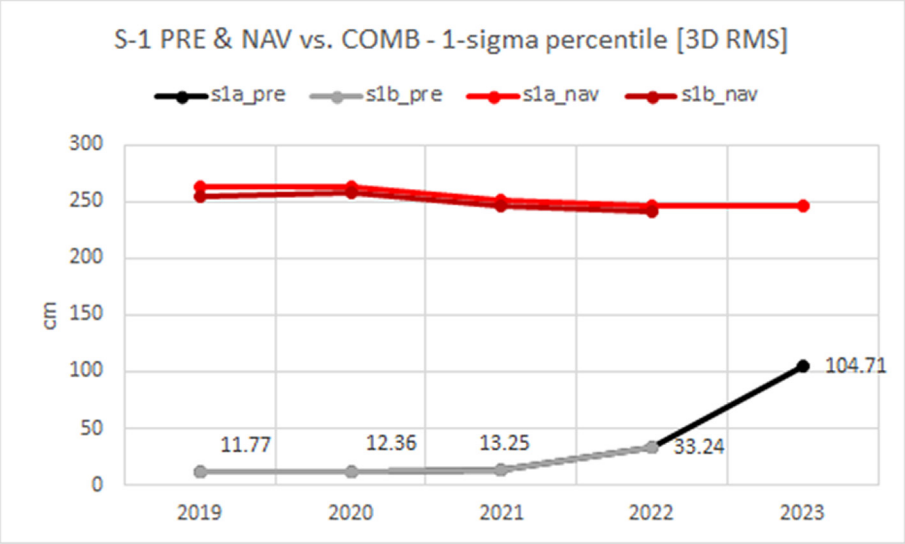

Fig. 17. Evolution of the 1-sigma of the 3D RMS of orbital accuracies of Sentinel-1 predicted and GNSS On-board navigation vs. combined products.

1 m in the first four months of 2023. However, the current accuracy is still below the nominal accuracy of the on-board GPS navigation solution (showed in Fig. 17 as compared also against the combined solution).

4.1.2. Near real time

The CPOD Service generates NRT restituted orbits for all the four Sentinel missions considered here. The term NRT refers to the short latency (see Table 3) available to generate the product once the GNSS data is available at the CPOD Service. Fig. 18 shows the 3D RMS of the differences between each product and the combined solution since the beginning of each mission. To better visualize the evolution of the accuracy over the years, Fig. 19 shows the 1-sigma of the 3D RMS (left) and radial component (right) (per product), considering all comparisons in each year. There are three features worth to comment:

1. The 1-sigma of 3D RMS of Sentinel-1 A&B have a sharp decrease in year 2020 due to the configuration change of the location of the GNSS antenna reference point, after confirming with the Sentinel-1 project that the documentation was ambiguous about the meaning of reference point. For more information about this change, see (Fernández et al., 2022).
2. There is a small, but clear decrease in the accuracy over the years 2022 and 2023, more clearly seen in the radial component, which is understood as a side effect of the increasing solar activity. For Sentinel-3 it is in the order of 5 mm in the radial component when comparing 2022 and 2023, but most of the jump is in 2023 (which in this analysis just refer to the first four month of the year), which has suffered several solar storms. It is known that the high solar activity has two main side effects for POD: an increased density of the atmosphere, which degrades the modelling of the satellite´s drag, and the increase of ionospheric scintillation, particularly over the polar regions, that causes an increased GNSS phase noise (see (Fernández et al., 2022) for a description of this last effect on the reprocessing of Sentinel-1). The increasing solar activity has less impact on Sentinel-6 MF due to the higher orbit compared to Sentinel-3.
3. There are differences between missions. Sentinel-1 and −2 seem to have better results than Sentinel-3 and −6; however, this is mostly a side effect of the different coverage of the NRT products. The NRT products of Sentinel-3 and −6 consist of the last orbit, and therefore they are more affected by boundary degradations in the POD batch processing, while the coverage analysed of Sentinel-1 goes from the last ascending node present in the GNSS data, one orbits backwards, which excludes the last part of the GNSS data available (the boundary). Finally, the coverage analysed of Sentinel-2 contains two orbits, but approximately half of the products includes the boundary of the GNSS data available, as with Sentinel-3 and −6, so that explain why it is slightly worse than Sentinel-1 (at least in the radial component). Indeed, a closer look at Sentinel-2A in year 2022 shows that by comparing only the last orbit, instead of two, the 1-sigma of 3D RMS goes from 2.95 cm (with two orbits) to 3.45 cm (with one orbit) and in radial RMS goes from 1.11 cm (with two orbits) to 1.32 cm (with one orbit), showing clearly the effect of the coverage assessed in the 1-sigma statistics.

4.1.3. Non time critical

The most accurate products generated routinely (excluding reprocessed solutions) are the NTC products. Fig. 20 shows the evolution of the 3D RMS of the NTC products of Sentinel-1 and Sentinel-3; in this plot, each dot represents one day. Fig. 21 shows the evolution of the 1-sigma

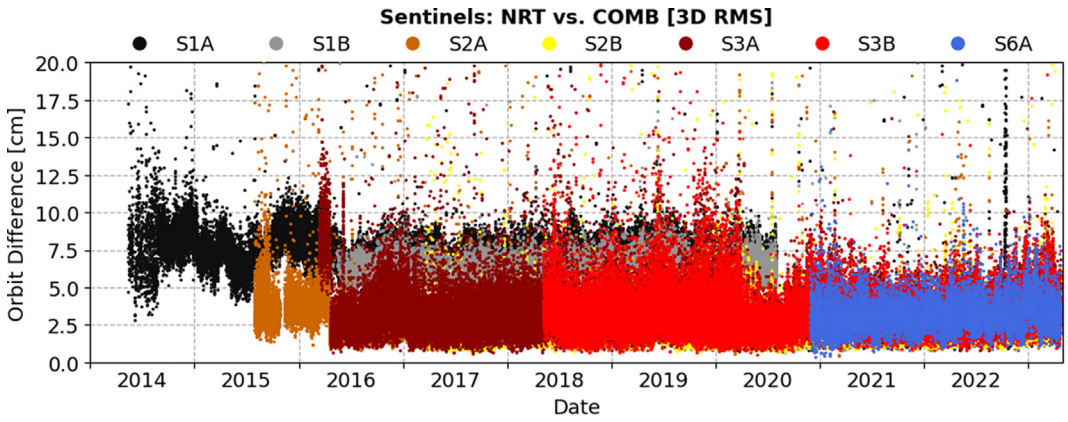

Fig. 18. Differences between CPOD NRT products and COMB solution in 3D RMS for Sentinel-1, −2, −3, and −6 missions.

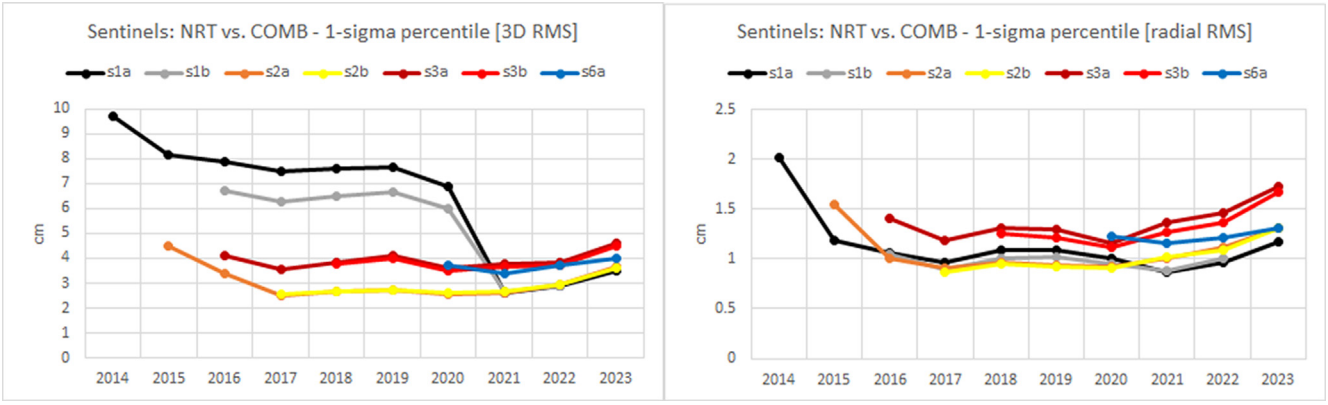

Fig. 19. Evolution of the 1-sigma of the 3D RMS (left) and radial (right) of orbital accuracies of NRT vs. combined products.

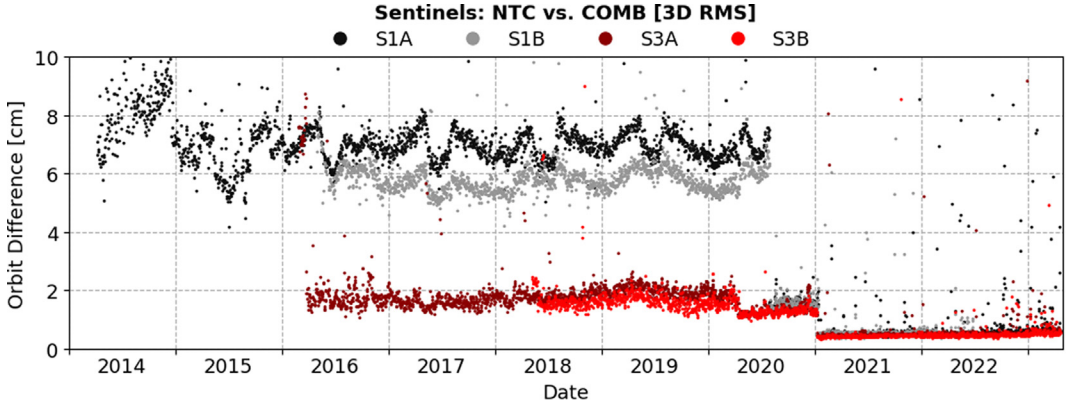

Fig. 20. Differences between CPOD NTC products and COMB solution in 3D RMS for Sentinel-1, and −3 missions.

of the 3D RMS (left) and radial RMS (right) per year. There are three features worth to comment:

1. As explained above, the jump of Sentinel-1 on year 2020 is due to the configuration change of the location of the GNSS antennas, which triggered the reprocessing of Sentinel-1 (visible in Fig. 23).
2. In the radial RMS a slight degradation of the accuracy of 1 mm can be seen in year 2023 that can only be understood as a side effect of the increased solar activity.
3. There are two clear improvements in the evolution of Sentinel-3 (better seen in Fig. 20), the first in April 2020 caused by the introduction of the new gravity field, ocean tides, and the use of ambiguity resolution, and the

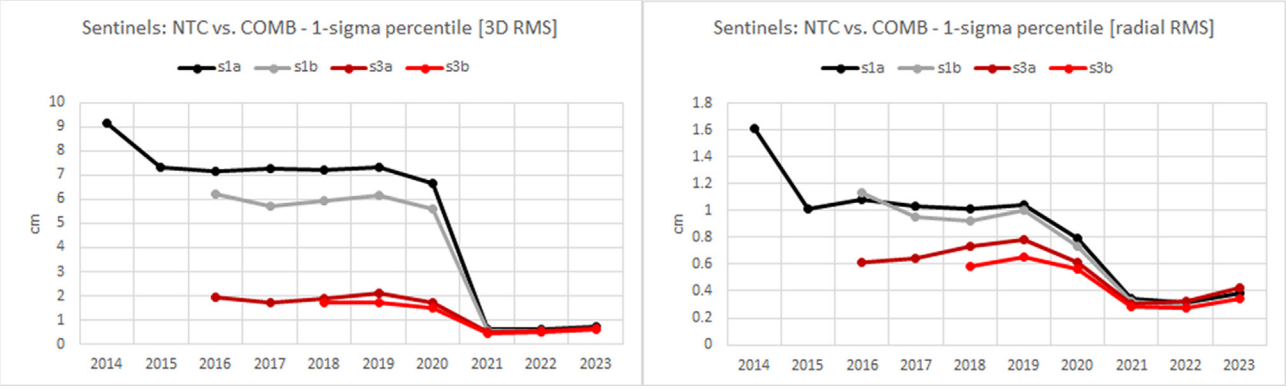

Fig. 21. Evolution of the 1-sigma of the 3D RMS (left) and radial (right) of orbital accuracies of NTC vs. combined products.

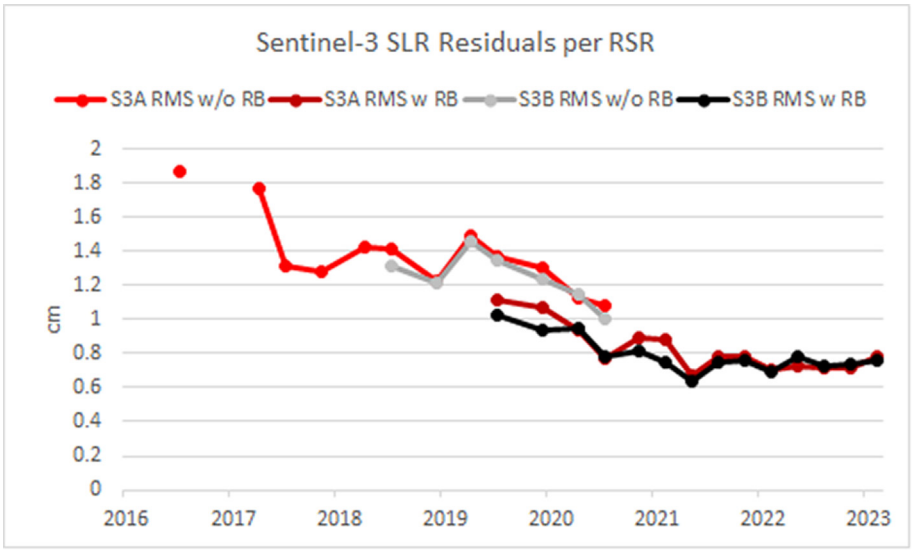

Fig. 22. Mean and RMS of the SLR residuals of the S-3 NTC orbit product per RSR period.

second in January 2021 caused by the use of a more reduce dynamic parametrization (see section 3.5.1). Sentinel-1 also benefits similarly of these configuration changes, but the first change is not visible due to the antenna location issue mentioned above.

Fig. 22 shows the SLR residuals of Sentinel-3 A&B, obtained during the elaboration of the RSRs from 2016 onwards. In the plot, every dot corresponds to the RMS over the period covered by the corresponding RSR (i.e., between 3 and 4 months). The figure shows two groups of curves, as from 2016 to 2019, no station range bias (RB) was removed, while afterwards a range bias per station was estimated for the period reported in the RSR, using the combined solution as the reference. Therefore, the red and grey curves correspond to S-3A & B without applying any range bias, and the dark red and black after correcting for the range biases. There is a period between 2019 and 2020 with an overlap between both metrics. The SLR residual analysis clearly shows the improvement thanks to the subsequent changes in the parametrization in year 2020 and 2021.

4.1.4. NRT VS. NTC

To better visualize the differences between the NRT and NTC products, Fig. 23 shows the evolution of the 3D RMS of the differences between the respective products of Sentinel-1A and the combined solution. This plot also includes the reprocessing done after the change of GNSS antenna location. Fig. 24 shows the evolution of the 1-sigma of 3D RMS (left) and radial (right) of these three products on a yearly basis. There are two relevant things to comment:

1. The difference between NRT and NTC is 2 – 3 cm in 3D RMS, and less than 1 cm in radial. The accuracy of the NTC/REP is below 1 cm in 3D RMS, while the NRT is in the order of 3 cm.

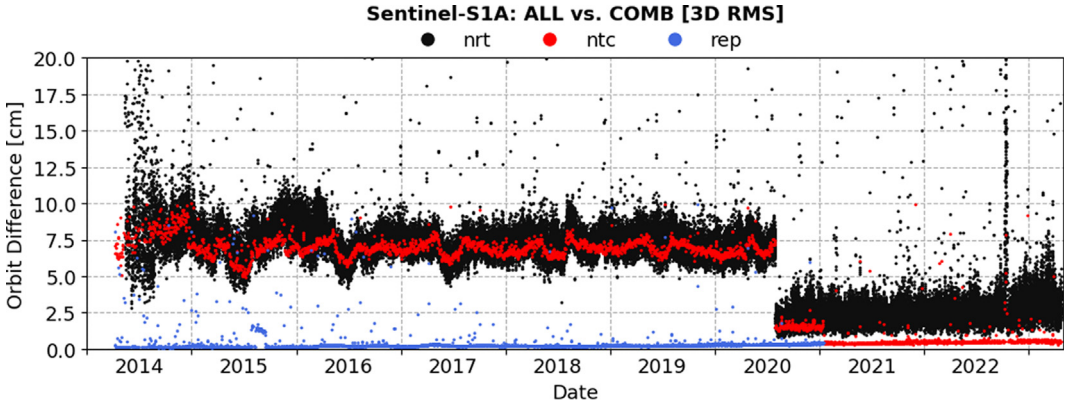

Fig. 23. Differences between CPOD Sentinel-1A products and COMB solution in 3D RMS.

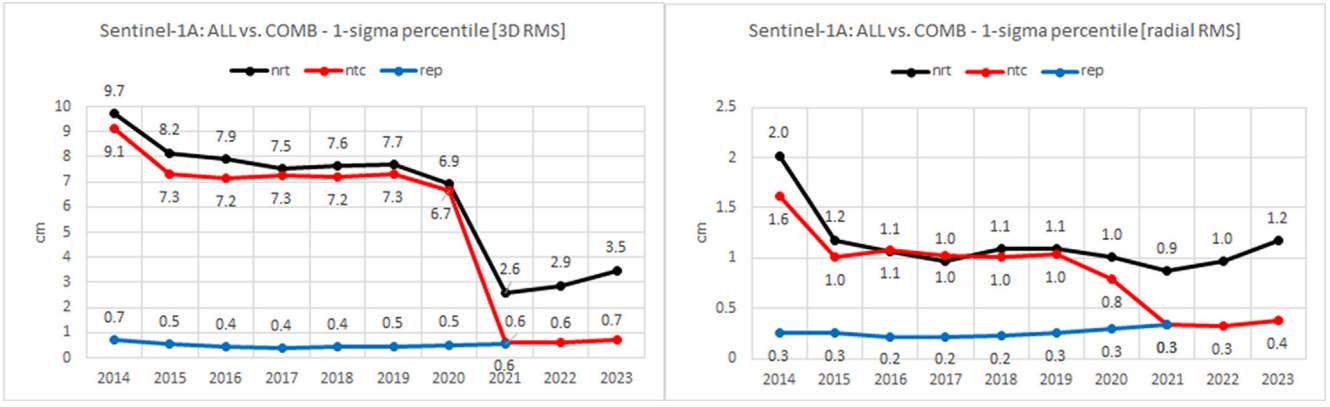

Fig. 24. Evolution of the 1-sigma of the 3D RMS (left) and radial (right) of orbital accuracies of Sentinel-1A products vs. combined orbit.

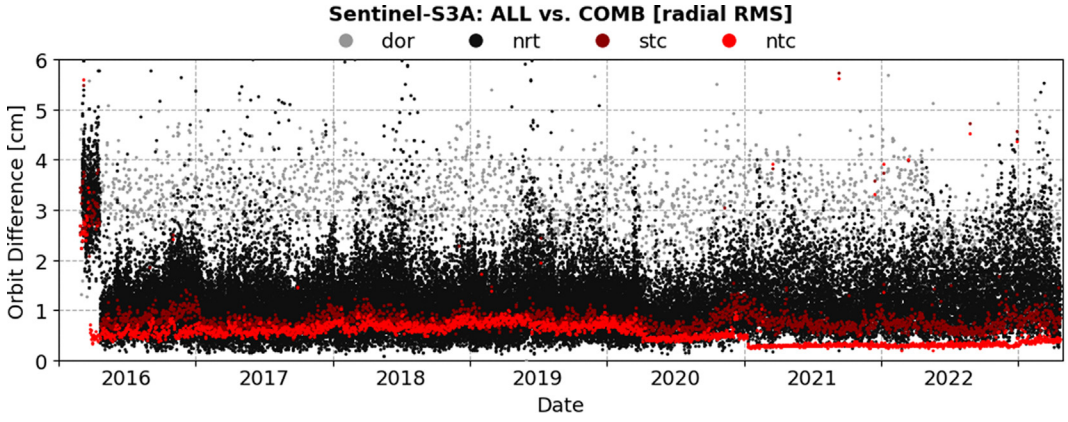

Fig. 25. Differences between Sentinel-3A orbit products and COMB solution in radial RMS.

2. The differences vs. the combined of the NTC/REP is increased over time, due to the ageing of the gravity field. See Berzosa et al. (2023).
3. The differences vs. the combined of the NRT is also increasing over the last years, particularly for year 2023, due to the higher solar activity.

The Sentinel-3 mission uses several orbit solutions for the altimetry processing. Fig. 25 shows the evolution over time of the radial RMS (which is the metric of interest for altimetry missions). The top figure shows four solutions: the DORIS on-board navigation solution, computed in real-time, and the NRT, STC and NTC solutions com-

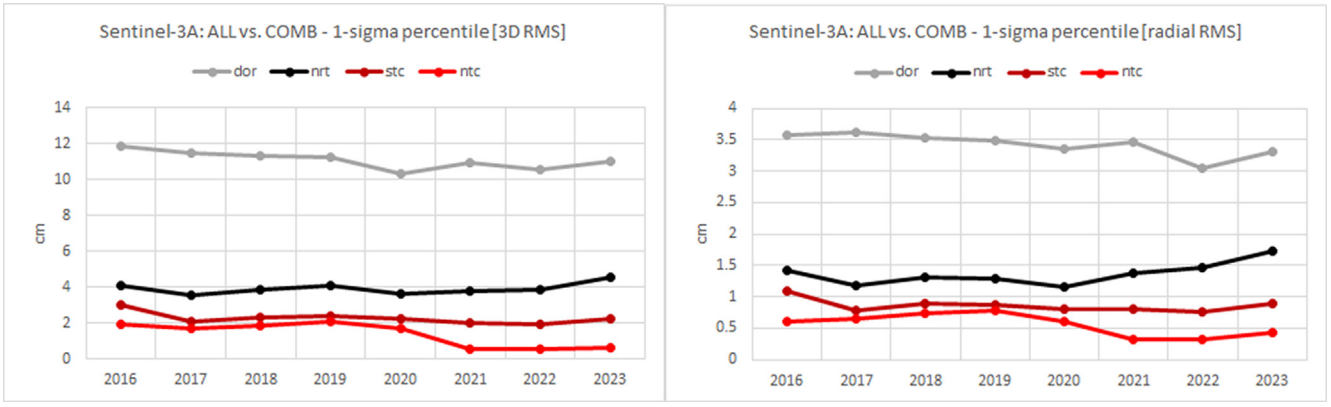

Fig. 26. Evolution of the 1-sigma of the 3D RMS (left) and radial (right) of orbital accuracies of Sentinel-3A products vs. combined orbit.

puted by the CPOD Service. Fig. 26 shows the evolution of the 1-sigma of 3D RMS (left) and radial (right) on yearly basis, of these products. It is worth to mention three things:

1. The radial difference between the DORIS on-board solution and the NRT solution, ranges from 2 cm between 2016 and 2021, and 1.5 cm in 2022 and 2023. The sub-daily differences are explained in section 4.3. The 3D differences are bigger than 6 cm due to the worse performance of DORIS on the along & cross-track directions.
2. The accuracy of the STC and NTC was pretty similar during the years 2017 to 2019, until the use of integer ambiguity resolution on the NTC product in 2020. Then, from 2021 onwards, the NTC solutions beat the STC by 5 mm, thanks to the use of a reduced-dynamic orbit and the integer ambiguity resolution. Year 2020 showed a slight improvement on the NTC with respect to STC, but the real benefit of the ambiguity resolution (introduced in 2020) was not obtained until the parametrization was changed in 2021 on both, the STC and NTC.

4.2. Sentinel-1A

In this section, the sub-daily evolution of the differences with respect to the combined solution are described and analysed.

4.2.1. Daily differences

Fig. 27 shows the sub-daily evolution of the differences between the NRT products generated on day 01/01/2022 and the combined solution. Each NRT product has a coverage of one orbit (from the last ascending node present in the GNSS data, one orbits back), and each product is generated independently using a 24 h determination arc. Considering that the NRT product is extracted from the right-hand side of the determination arc, any mis-modelling on the drag, potential the lack of accurate GNSS products in the last 15 min of the determination interval, and the lack of additional data afterwards, will have an impact on the orbital accuracy. This justifies the clear jumps visible in the figure, which correspond to the jump between two consecutive products. The total component (in red) never

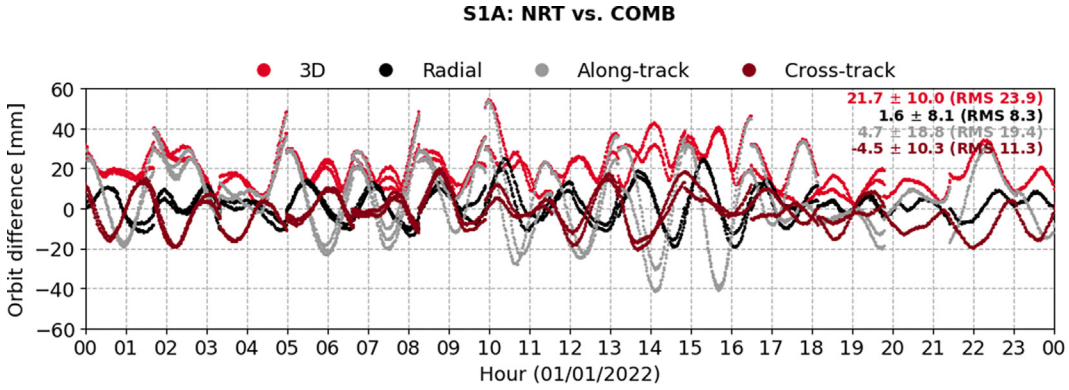

Fig. 27. Temporal evolution of orbit differences between S-1A NRT and COMB solutions on day 01/01/2022.

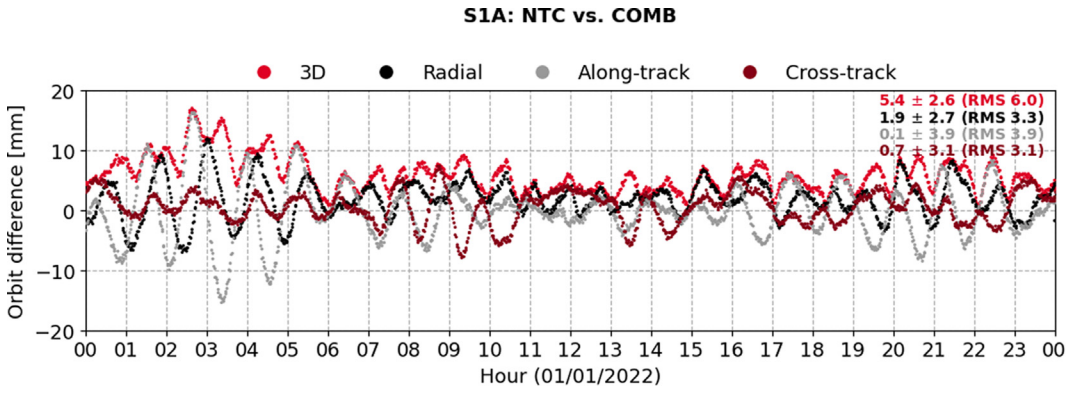

Fig. 28. Temporal evolution of orbit differences between S-1A NTC and COMB solutions on day 01/01/2022.

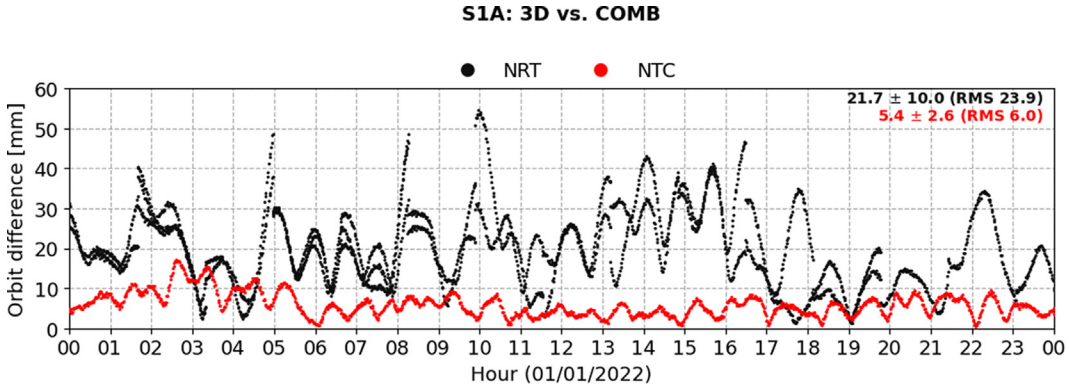

Fig. 29. Temporal evolution of 3D RMS differences between S-1A NRT & NTC and COMB solutions on day 01/01/2022.

exceeds the 6 cm in this case, while the total RMS is just 2.39 cm.

Fig. 28 shows the sub-daily evolution of the differences between the NTC product of day 01/01/2022 and the combined solution. Compared with the previous figure, the y-axis here is 3 times smaller, and the amplitude of the total component (in red) never exceeds 2 cm, with a total RMS of just 6 mm.

Fig. 29 summarizes the previous discussion showing the sub-daily evolution of the 3D differences between the NRT and NTC vs. the combined solution. It can be clearly seen that the NTC differences (in red) are not only smaller but they lack the jumps between products which is unavoidable on the NRT.

Finally, Fig. 30 shows two interesting metrics:

1. A geographical plot in the left, showing the 3D RMS of the differences between Sentinel-1A NTC and the combined solution, considering the months from January to April 2022. The plot shows some signals which seems to be isolated orbits, rather than systematic patterns in the plot. To generate this plot some big outliers have

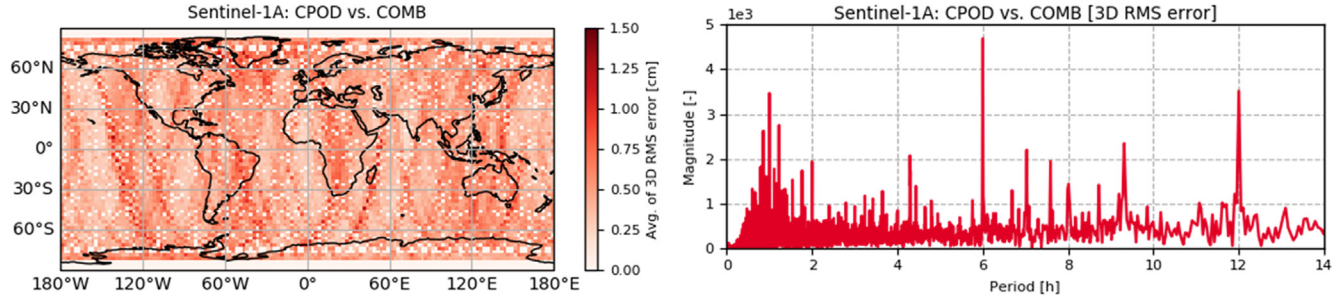

Fig. 30. Geographical (left) and spectral analysis (right) of Sentinel-1A NTC solution over the period Jan-Apr 2022.

been excluded, but considering the amplitude of the values, with a maximum of 1.5 cm, and that Sentinel-1 manoeuvres on weekly or bi-weekly basis, these features could be related with remaining outliers. But it cannot be disregarded that the gravity field is ageing (Berzosa et al., 2023) and some geographical features (e.g., over Greenland) are more related to the gravity field.

2. A Fourier analysis of the orbit differences shows clear spectral lines at 6 h and 12 h, but also around 1 h. Considering that the parametrization uses empirical accelerations every 2 h, it is not a surprise to find spectral lines of multiple of it (like 6 and 12), but it is a surprise that the spectral line at 2 and 4 h are very small. So far, no clear explanation for these signals have been found.

4.2.2. Change of models

Since 2020, there have been three significant changes on the parametrization of the Sentinel-1 mission. To visualize the impact of these changes on the sub-daily evolution of the differences with respect to the combined solution, Fig. 31 shows three figures:

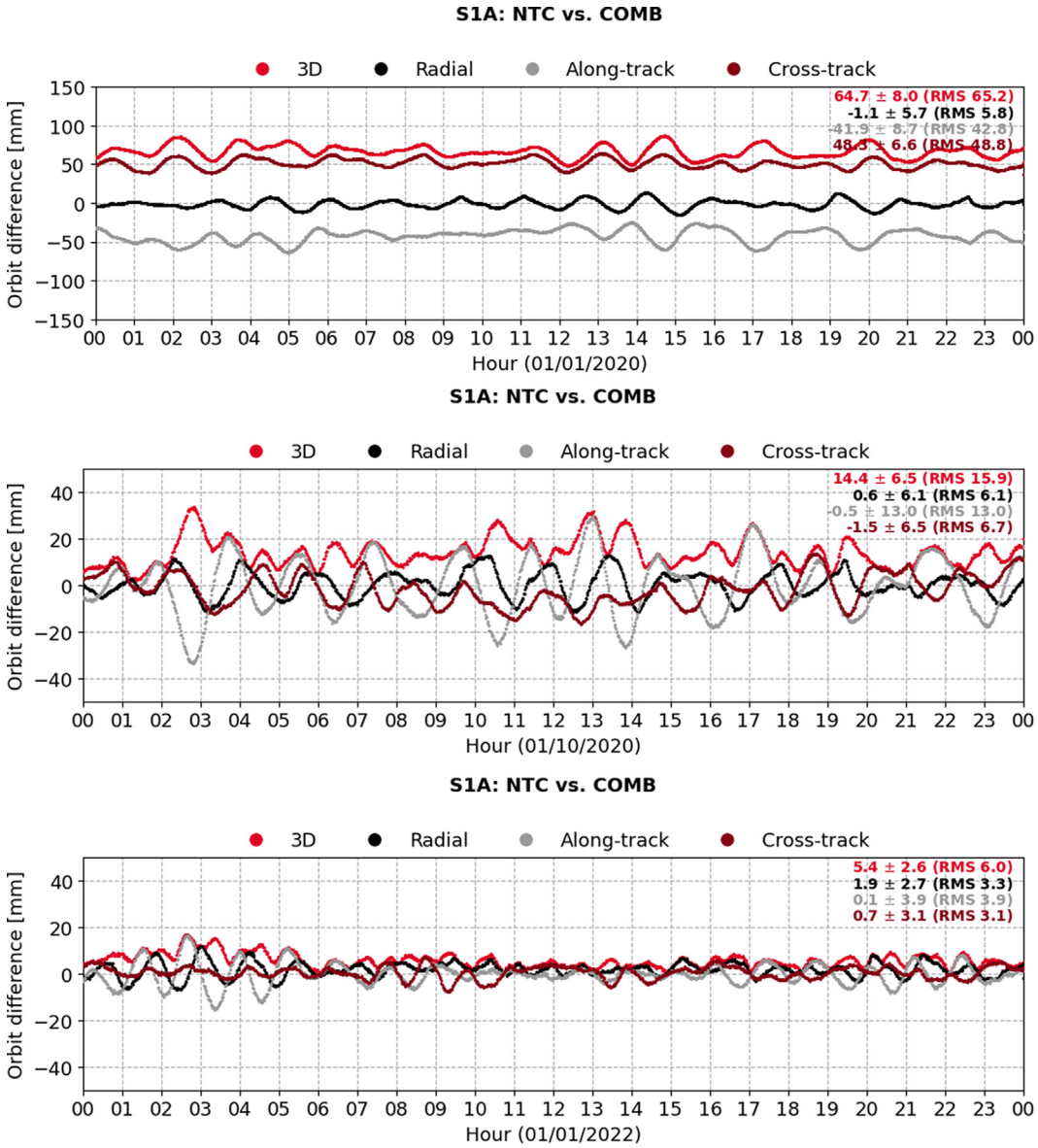

Fig. 31. Temporal evolution of orbit differences between S-1A NTC and COMB solutions on days 2020/01/01 (top), 2020/10/01 (mid) and 2022/01/01 (below).

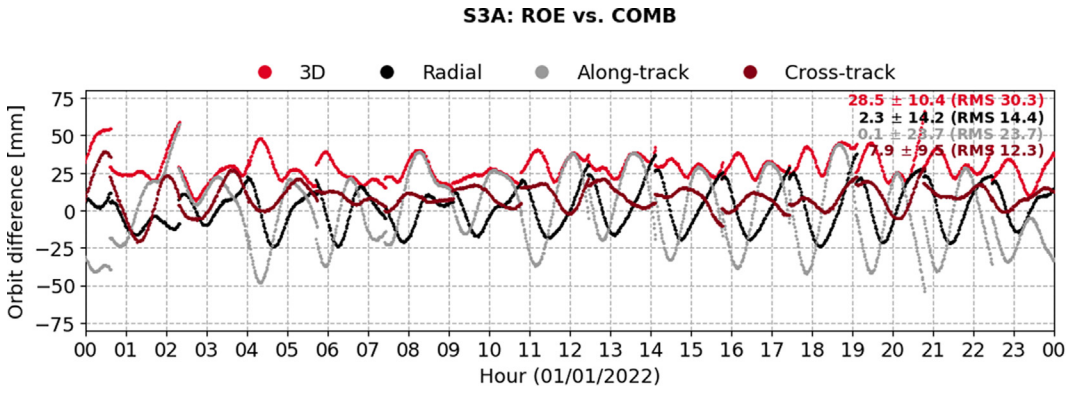

Fig. 32. Temporal evolution of orbit differences between S-3A NRT and COMB solutions on day 01/01/2022.

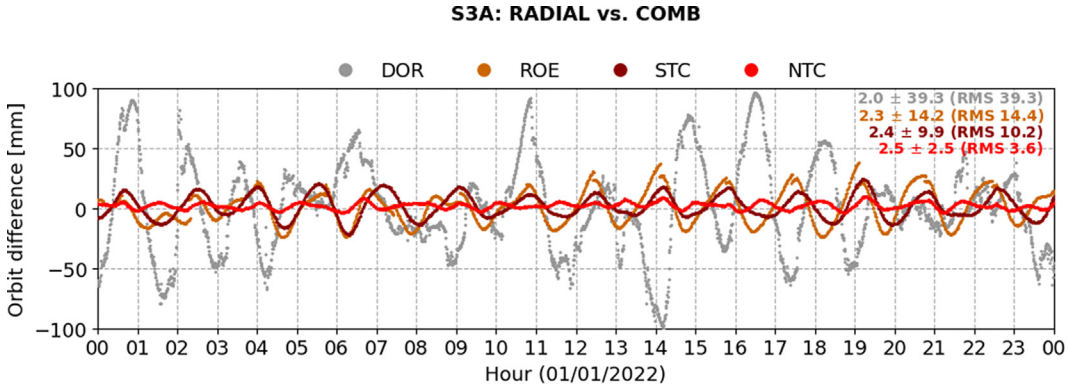

Fig. 33. Temporal evolution of radial orbit differences between S-3A and COMB solutions on day 01/01/2022.

1. The top image corresponds to the case where the incorrect location of the GNSS antenna was still used. The location was wrong by few cm in the along and cross-track directions, so this plot clearly visualize these biases in these components.
2. The middle image corresponds to an epoch after correcting the location of the GNSS antenna, and after changing the parametrization to resolve the integer ambiguities and to update the gravity field and ocean tides models. In this case, the total 3D RMS is just 15.9 mm.
3. The images at the bottom corresponds to an epoch using the parametrization currently used, which is significantly more reduced-dynamic than the previous one. It clearly shows the improvement over the previous parametrization. In terms of 3D RMS, it goes from 15.9 to 6 mm.

4.3. Sentinel-3A

4.3.1. Daily differences

Fig. 32 shows the sub-daily evolution of the differences between the NRT products generated on day 01/01/2022 and the combined solution. Each NRT product has a coverage of one orbit, and each of them is generated independently, using a 24 h determination arc, where the last part covered in the determination arc is the coverage of the product, so it is affected by mis-modelling on the drag, possible lack of accurate GNSS products in the last 15 min of the determination interval, and the lack of additional data afterwards. This justifies the clear jumps visible in the figure, which correspond to the jump between two consecutive products. The radial component (in black) never exceeds 4 cm in this case and exhibit a clear pattern with orbital frequency, while the radial RMS is 14.4 mm.

Fig. 33 shows the radial differences between four different products: the DORIS On-board Navigation Solution, and the CPOD products ROE (the NRT), STC and NTC, on day 01/01/2022. It shows the sub-daily differences between these products, with radial RMS of 39.3 mm for the DORIS, 14.4 mm for the ROE, 10.2 mm for the STC and 3.6 mm for the NTC. While all exhibit a clear orbital pattern, the DORIS on-board solution has amplitudes that reaches 10 cm, while the ROE never reaches 5 cm. The STC solution is slightly

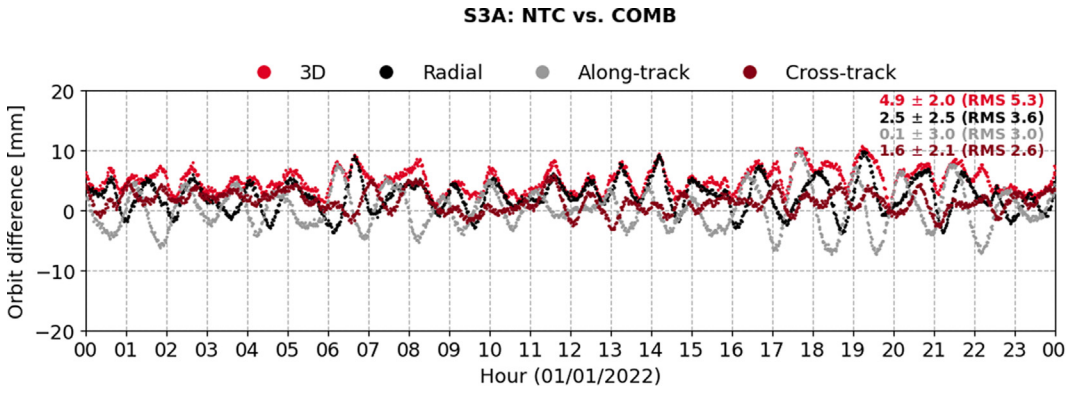

Fig. 34. Temporal evolution of orbit differences between S-3A NTC and COMB solutions on day 01/01/2022.

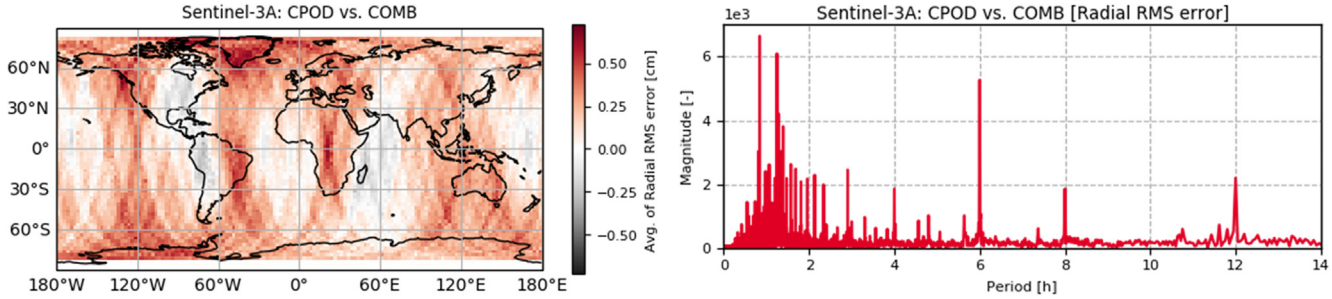

Fig. 35. Geographical (left) and spectral analysis (right) of Sentinel-3A NTC solution over the period Jan-Apr 2022.

better than the ROE, and obviously lacks the jumps present in the ROE.

Fig. 34 shows the evolution of the differences between the NTC and the combined solution for Sentinel-3A on day 01/01/2022. The differences just reach 1 cm in the worst case, and exhibit a 2.5 mm bias in the radial component, with 3.6 mm of radial RMS.

Fig. 35 shows the radial orbit errors in a geographical plot (left) and a spectral plot (right), considering all differences between January and April 2022. The geographical plot shows clear geographical patterns (e.g., over Greenland), that could be due to the ageing of the gravity field used (Berzosa et al., 2023). Meanwhile, the spectral plot shows clear signals on the 4, 6, 8 and 12 h, and also below 2 h which are not discussed here. It is thought that these spectral lines should be related with the reduced-dynamic orbit parametrization that uses empirical accelerations every 2 h. However, it is interesting that there is no line at 10 h.

4.3.2. Change of models

Like with the discussion of Sentinel-1 in section 4.2.2 there has been three significant changes since 2020 in the parametrization of the Sentinel-3 orbit. To visualize the impact of these changes on the sub-daily evolution of the differences with respect to the combined solution, Fig. 36 shows three figures:

1. The image at the top corresponds to the parametrization that was not resolving the integer ambiguity. In this case, the radial component has amplitudes that reach 2 cm, and an RMS of 6.6 mm.
2. The middle image corresponds to an epoch after starting to resolve the integer ambiguity and updating the gravity field and ocean tides models. In this case, the radial RMS is reduced slightly to 4.9 mm, but the sub-daily differences still have amplitudes close to 2 cm.
3. The image at the bottom corresponds to an epoch using the parametrization currently used, which is significantly more reduced-dynamic than the previous one. It clearly shows the improvement over the previous parametrization. The radial RMS is significantly better than the other two cases, being 3.6 mm, with maximum amplitudes of 1 cm. However, this parametrization shows a clear radial bias of 2.5 mm, that was not present in the previous cases (probably due to the higher errors), that indicates that there is still work to be done.

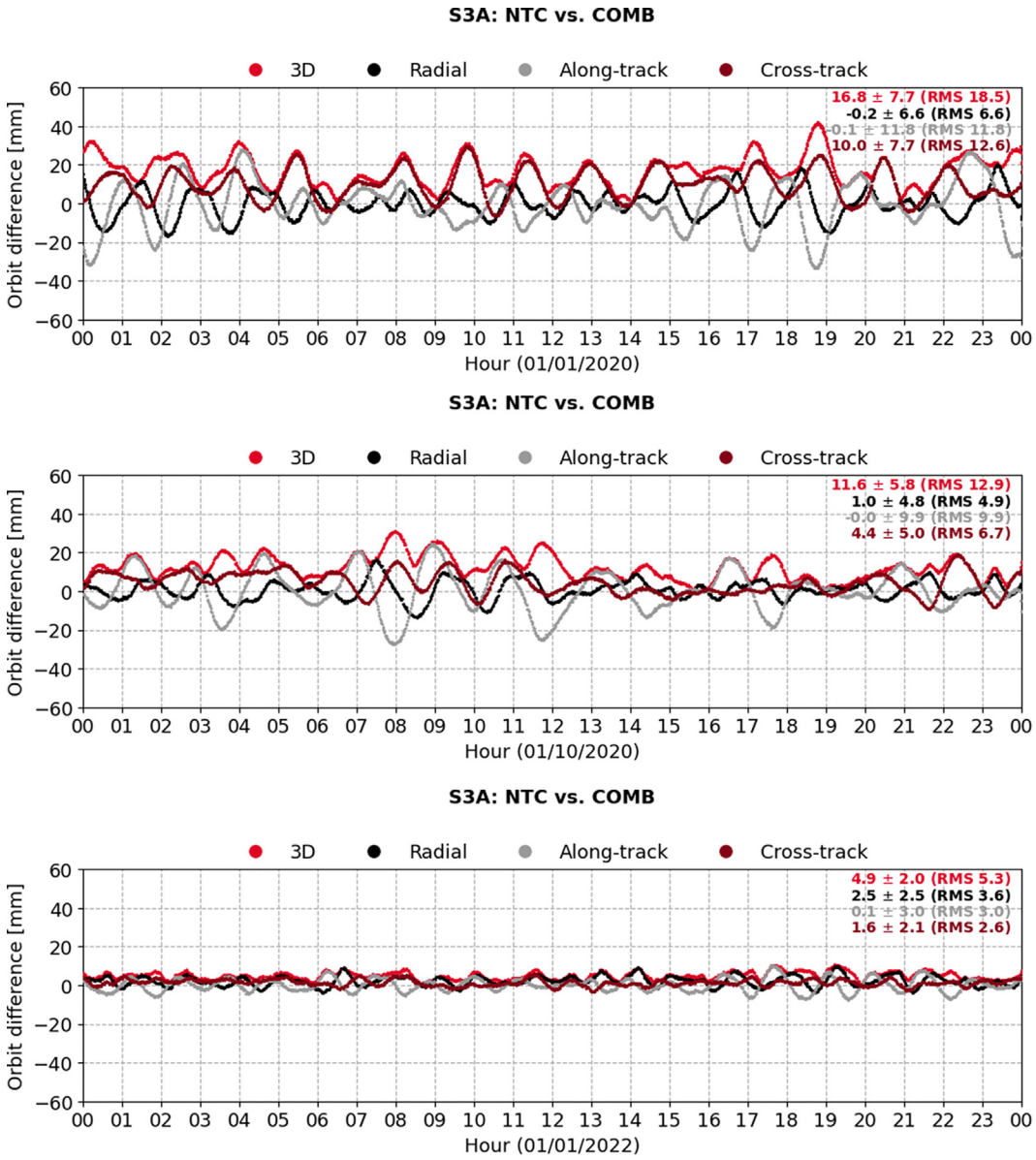

Fig. 36. Temporal evolution of orbit differences between S-3A NTC and COMB solutions on days 01/01/2020 (top), 01/10/2020 (mid) and 01/01/2022 (below).

5. Conclusions and way forward

This paper has provided a thorough review of the CPOD Service in terms of missions supported, its physical and logical design, the evolutions of the POD algorithms since 2013, and finally has presented the accuracy of the orbit products as compared to a combined solution, but also using SLR data when available. In terms of architecture, the CPOD Service has evolved significantly over the last years to be faster to provide the final products. In terms of accuracy, and thanks to the CPOD QWG, the CPOD Service has carried out significant enhancements on the POD parametrization to reach the current remarkable level of accuracy which goes significantly beyond the initial accuracy requirements. The CPOD Service is also committed to provide support to external users, by providing GNSS data, and POD products, but also publishing ancillary data and documentation that allow external users to carry out their own investigations or services.

In January 2023, the CPOD Service initiated its third renovation, with a significant change. After 9 years of operations using NAPEOS, the service changed to use a new GMV´s proprietary SW called ***FocusPOD*** (Fernández et al., 2023). While in terms of POD algorithms, ***FocusPOD*** is in line with NAPEOS, in terms of SW architecture it is quite more flexible and faster. This new SW will allow deploying new operational schemes to be more reactive and faster to deliver products and metrics, always maintaining the quality of the products. In terms of POD parametrization, the most urgent change will be the geopo-

tential model, as the model used currently shows clear signs of ageing. One possibility is to use the COST-G FSM (Fitted Signal Model, Peter et al., 2022). Other potential improvements will come from improvements on the solar radiation pressure models (particularly for Sentinel-6), and with the use of integer ambiguity resolution in STC, to try to obtain accuracies similar to those obtained in NTC. Finally, the impact of the higher solar activity has to be investigated further to try to minimize its impact.

The Sentinel-1, −2, −3, and −6 GNSS, attitude data, and operational products are available on the Copernicus Data Space Ecosystem (https://dataspace.copernicus.eu). Support information for the processing is available on the Sentinels Online:

- S1: https://sentinels.copernicus.eu/web/sentinel/technical-guides/sentinel-1-sar/pod
- S2: https://sentinels.copernicus.eu/web/sentinel/technical-guides/sentinel-2-msi/pod
- S3: https://sentinels.copernicus.eu/web/sentinel/technical-guides/sentinel-3-altimetry/pod

And for S6: https://www.eumetsat.int/sentinel-6-data.

CRediT authorship contribution statement

Jaime Fernández: Writing – original draft. **Heike Peter:** Writing – review & editing.

Declaration of competing interest

The authors declare that they have no known competing financial interests or personal relationships that could have appeared to influence the work reported in this paper.

Acknowledgements

The CPOD Service is financed under ESA contract No. 4000139509/22/I-BG, which is gratefully acknowledged. The work performed in the frame of this contract is carried out with funding by the European Union. The views expressed herein can in no way be taken to reflect the official opinion of either the European Union or the European Space Agency. The authors also acknowledge the work done by the CPOD QWG, which provides the precise orbits of the Sentinels needed to generate the combined solution, and are a constant source of knowledge and inspiration to improve the CPOD Service. The provision of GNSS orbit, clock, and biases products by the IGS and particularly by CODE, and SLR data by the ILRS is also greatly appreciated.

References

Aschbacher, J., Milagro-Pérez, M., 2012. The European earth monitoring GMES programme: Status and perspectives. Remote Sens. Environ. 120, 3–8. https://doi.org/10.1016/j.rse.2011.08.028.

Bancroft, S. 1985. An algebraic Solution of the GPS Equations. IEEE transactions on aerospace and electronic systems. AES-21(1), 56-59. https://doi.org/10.1109/TAES.1985.310538.

Bertiger, W., Desai, S.D., Haines, B., Harvey, N., Moore, A.W., Owen, S., Weiss, J.P., 2010. Single receiver phase ambiguity resolution with GPS data. J Geod 84, 327–337. https://doi.org/10.1007/s00190-010-0371-9.

Bertiger, W., Bar-Sever, Y., Dorsey, A., Haines, B., Harvey, N., Hemberger, D., Heflin, M., Lu, W., Miller, M., Moore, A.W., Murphy, D., Ries, P., Romans, L., Sibois, A., Sibthorpe, A., Szilagyi, B., Vallisneri, M., Willis, P., 2020. GipsyX/RTGx, a new tool set for space geodetic operations and research. Adv. Space Res. 66 (3), 469–489. https://doi.org/10.1016/j.asr.2020.04.015.

Berzosa, J., Fernández, C., Muñoz, M.A., Fernández, M., Fernández, J., Peter, H., Meyer, U., Féménias, P., Nogueira, C. 2023. Reprocessing of Copernicus Sentinel POD solutions with COST-G geopotential. Poster at EGU General Assembly 2023 23-28 April 2023, Vienna, Austria. https://doi.org/10.5194/egusphere-egu23-16137.

Berzosa, J., Peter, H., Fernández, J., Féménias, P., 2021. Copernicus Sentinel-3B – GPS L2C tracking tests during commissioning phase. Adv Space Res 68 (2), 1023–1047. https://doi.org/10.1016/j.asr.2019.11.017.

Beutler, G., Kouba, J., Springer, T.A., 1995. Combining the orbits of the IGS analysis centers. Bulletin Géodésique 69, 200–222. https://doi.org/10.1007/BF00806733.

Bock, H., Jäggi, A., Beutler, G., Meyer, U., 2014. GOCE: precise orbit determination for the entire mission. J Geod 88, 1047–1060. https://doi.org/10.1007/s00190-014-0742-8.

Bosch, W., Savcenko, R. 2007. Satellite Altimetry: Multi-Mission Cross Calibration. In: Tregoning, P., Rizos, C. (Eds.), Dynamic Planet. International Association of Geodesy Symposia, vol 130. Springer, Berlin, Heidelberg. https://doi.org/10.1007/978-3-540-49350-1_8.

Bosch, W., Dettmering, D., Schwatke, C., 2014. Multi-mission cross-calibration of satellite altimeters: Constructing a long-term data record for global and regional sea level change studies. Remote Sens. (Basel) 6 (3), 2255–2281. https://doi.org/10.3390/rs6032255.

Carrou, J.P. 1986. Zoom Software: Error Analysis and Accurate Orbit Restitution at CNES, In: Bhatnagar, K.B. (Eds.), Space Dynamics and Celestial Mechanics. Astrophysics and Space Science Library, vol 127. Springer, Dordrecht. https://doi.org/10.1007/978-94-009-4732-0_36.

CNES/CLS, 2023. CNES/CLS Analysis Center for IDS. Available at https://idsac-cnes.cls.fr/index.html, last access: 05 Jan 2024.

Conrad, A., Axelrad, P., Desai, S., Haines, B. 2022. Improved Modeling of the Solar Radiation Pressure for the Sentinel-6 MF Spacecraft. In: Proceedings of the 35th International Technical Meeting of the Satellite Division of The Institute of Navigation (ION GNSS+ 2022), Denver, Colorado, September 2022, pp. 3618-3631. https://doi.org/10.33012/2022.18478.

Dach, R., Lutz, S., Walser, P., Fridez, P. 2015. Bernese GNSS software version 5.2. Technical Report. Astronomical Institute, University of Bern. https://doi.org/10.7892/boris.72297.

Dach, R., Schaer, S., Arnold, D., Kalarus, M.S., Prange, L., Stebler, P., Jäggi, A., Villiger, A. 2020a. CODE final product series for the IGS. Published by Astronomical Institute, University of Bern. http://www.aiub.unibe.ch/download/CODE. https://doi.org/10.7892/boris.75876.4.

Dach, R., Schaer, S., Arnold, D., Kalarus, M.S., Prange, L., Stebler, P., Villiger, A., Jäggi, A. 2020b. CODE rapid product series for the IGS. Published by Astronomical Institute, University of Bern. http://www.aiub.unibe.ch/download /CODE. https://doi.org/10.7892/boris.75854.4.

Debaisieux, A., Aubry, J.P., Gerard, E., Brunet, M. 1985. A satellite oscillator for very precise orbitography: The DORIS program. In: 39th

Annual Symposium on Frequency Control. Philadelphia, PA, USA pp. 202-211. https://doi.org/10.1109/FREQ.1985.200846.

Dobslaw, H., Bergmann-Wolf, I., Dill, R., Poropat, L., Thomas, M., Dahle, C., Esselborn, S., König, R., Flechtner, F., 2017. A new high-resolution model of non-tidal atmosphere and ocean mass variability for de-aliasing of satellite gravity observations: AOD1B RL06. Geophys. J. Int. 211 (1), 263–269. https://doi.org/10.1093/gji/ggx302.

Donlon, C.J., Cullen, R., Giulicchi, L., Vuilleumier, P., Francis, C.R., Kuschnerus, M., Simpson, W., Bouridah, A., Caleno, M., Bertoni, R., Rancaño, J., Pourier, E., Hyslop, A., Mulcahy, J., Knockaert, R., Hunter, C., Webb, A., Fornari, M., Vaze, P., Brown, S., Willis, J., Desai, S., Desjonqueres, J.D., Scharroo, R., Martin-Puig, C., Leuliette, E., Egido, A., Smith, W.H.F., Bonnefond, P., Le Gac, S., Picot, N., Tavernier, G., 2021. The Copernicus Sentinel-6 mission: enhanced continuity of satellite sea level measurements from space. Remote Sens Environ 258. https://doi.org/10.1016/j.rse.2021.112395 112395.

Duan, B., Hugentobler, U., 2021. Comparisons of CODE and CNES/CLS GPS satellite bias products and applications in Sentinel-3 precise orbit determination. GPS Sol 25, 128. https://doi.org/10.1007/s10291-021-01164-5.

ESA Sentinel-2 team, 2012. Sentinel-2: ESA's optical high-resolution mission for GMES operational services. ESA SP-1322/2, ISBN 978-92-9221-419-7.

ESA Sentinel-3 team, 2012. Sentinel-3: ESA's global land and ocean mission for GMES operational services. ESA SP-1322/3, ISBN 978-92-9221-420-3.

ESA, 1992. ERS-1 System. ESA SP-1146, ISBN 92-9092-021-1.

Fernández, J., Escobar, D., Ayuga, F., Féménias, P., 2016. Copernicus POD operational experience. In: 14th International Conference on Space Operations (SpaceObs 2016) May 16-20, 2016, Daejeon, Korea. https://doi.org/10.2514/6.2016-2385.

Fernández, J., Escobar, D., Águeda, A., Féménias, P. 2014. Sentinels POD Service Operations. Proceedings of 13th International Conference on Space Operations (SpaceOps 2014), May 5-9, 2014, Pasadena, CA, United States. https://doi.org/10.2514/6.2014-1929.

Fernández, J., Escobar, D., Peter, H., Féménias, P. 2015a. Copernicus POD Service Operations – Orbital accuracy of Sentinel-1A and Sentinel-2A. Proceedings of 25th International Symposium on Space Flight Dynamics ISSFD2015. October 19-23, 2015, Munich, Germany.

Fernández, J., Escobar, D., Ayuga, F., Peter, H., Féménias, P. 2015b. Sentinels POD Service Operations. Proceedings of Sentinel-3 for Science Workshop, June 2-5, 2015, Venice, Italy. ESA SP-734.

Fernández, J., Peter, H., Calero, E.J., Berzosa, J., Gallardo, L.J., Féménias, P. 2019. Sentinel-3A: Validation of Orbit Products at the Copernicus POD Service. In: Mertikas, S., Pail, R. (Eds.), Fiducial Reference Measurements for Altimetry. International Association of Geodesy Symposia, vol 150. Springer, Cham. https://doi.org/10.1007/1345_2019_64.

Fernández, C., Berzosa, J., Bao, L., Muñoz, M.A., Fernández, M., Lara, S., Terradillos, E., Fernández, J., Peter, H., Féménias, P., Nogueira, C. 2023. ***FocusPOD***, The new POD SW used at CPOD Service, EGU General Assembly 2023, Vienna, Austria, 24–28 Apr 2023, EGU23-1908, https://doi.org/10.5194/egusphere-egu23-1908.

Fernández, M., Peter, H., Arnold, D., Duan, B., Simons, W., Wermuth, M., Hackel, S., Fernández, J., Jäggi, A., Hugentobler, U., Visser, P., Féménias, P., 2022. Copernicus Sentinel-1 POD reprocessing campaign. Adv Space Res 70 (2), 249–267. https://doi.org/10.1016/j.asr.2022.04.036.

Fernández, J. 2022. Copernicus POD Service File Format Specification. Available at https://sentinels.copernicus.eu/web/sentinel/technical-guides/sentinel-3-altimetry/pod/documentation, last access: 5 Jan 2024.

Floberghagen, R., Fehringer, M., Lamarre, D., Muzi, D., Frommknecht, B., Steiger, C., Piñeiro, J., da Costa, A., 2011. Mission design, operation and exploitation of the gravity field steady-state and ocean circulation explorer mission. J Geod 85, 749–758. https://doi.org/10.1007/s00190-011-0498-3.

Folkner, W.M., Williams, J.G., Boggs, D.H. 2009. The Planetary and Lunar Ephemeris DE421. JPL Interplanetary Network Progress Report 42-178.

Förste, C., Flechtner, F., Schmidt, R., König, R., Meyer, U., Stubenvoll, R., Rothacher, M., Barthelmes, F., Neumayer, H., Biancale, R., Bruinsma, S., Lemoine, J.M. 2006. A Mean Global Gravity Field Model from the Combination of Satellite Mission and Altimetry/Gravimetry Surface Data. Geophysical Research Abstracts Vol. 8, 03462. Available at https://meetings.copernicus.org/www.cosis.net/abstracts/EGU06/03462/EGU06-J-03462-2.pdf, last access: 5 Jan 2024.

Friis-Christensen, E., Lühr, H., Knudsen, D., Haagmans, R., 2008. Swarm – an earth observation mission investigating geospacer. Adv Space Res 41 (1), 210–216. https://doi.org/10.1016/j.asr.2006.10.008.

Jäggi, A., Hugentobler, U., Beutler, G., 2006. Pseudo-stochastic orbit modelling techniques for low-earth orbiters. J Geod 80 (1), 47–60. https://doi.org/10.1007/s00190-006-0029-9.

Jäggi, A., Hugentobler, U., Bock, H., Beutler, G., 2007. Precise orbit determination for GRACE using undifferenced or doubly differenced GPS data. Adv Space Res 39 (10), 1612–1619. https://doi.org/10.1016/j.asr.2007.03.012.

Jäggi, A., Meyer, U., Lasser, M., Jenny, B., Lopez, T., Flechtner, F., Dahle, C., Förste, C., Mayer-Gürr, T., Kvas, A., Lemoine, J.M., Bourgogne, S., Weigelt, M., Groh, A., 2020. International combination Service for Time-Variable Gravity Fields (COST-G) – start of operational phase and future perspectives. In: Freymueller, J.T., Sánchez, L. (Eds.), Beyond 100: the next Century in Geodesy. IAG Symposia Series 152. Springer, Cham. https://doi.org/10.1007/1345_2020_109.

Johnston, G., Riddell, A., Hausler, G. 2017. The International GNSS Service. In: Teunissen, P., Montenbruck, O. (Eds.), Springer handbook of global navigation satellite systems. Springer, chap.33, 967-982. https://doi.org/10.1007/978-3-319-42928-1_33.

Kobel, C., Arnold, D., Jäggi, A., 2019. Combination of precise orbit solutions for Sentinel-3A using variance component estimation. Adv. Geosci. 50, 27–37. https://doi.org/10.5194/adgeo-50-27-2019.

Laurichesse, D., Mercier, F., Berthias, J.P., Broca, P., Cerri, L., 2009. Integer ambiguity resolution on undifferenced GPS phase measurements and its application to PPP and satellite precise orbit determination. Navigation 56 (2), 135–149. https://doi.org/10.1002/j.2161-4296.2009.tb01750.x.

Lemoine, J.M., Biancale, R., Reinquin, F., Bourgogne, S., Gégout, P., 2019. CNES/GRGS RL04 earth gravity field models, from GRACE and SLR data. GFZ Data Services. https://doi.org/10.5880/ICGEM.2019.010.

Lemoine, J.M., Bourgogne, S., Bruinsma, S., Reinquin, F., Gégout, P., Biancale, R. 2015. GDR-E Gravity Field Model EIGEN-GRGS. RL03-V2.Mean-Field. Ocean Surface Topography Science Team Meeting 2015. Available at https://ostst.aviso.altimetry.fr/fileadmin/user_upload/tx_ausyclsseminar/files/OSTST2015/POD-05-JMle-moine_Biancale_OSTST_POD.pptx.pdf, last access: 05 Jan 2024.

Louet, J. 2001 The Envisat Mission and System. ESA Bulletin No.106 (EnviSat Special Issue), 10-25. Available at https://www.esa.int/esapub/bulletin/bullet106/bul106_1.pdf, last access: 5 Jan 2024.

Lyard, F.H., Allain, D.J., Cancet, M., Carrère, L., Picot, N., 2021. FES2014 global ocean tides atlas: design and performance. Ocean Sci 17, 615–649. https://doi.org/10.5194/os-17-615-2021.

Lyard, F., Lefevre, F., Letellier, T., Francis, O., 2006. Modelling the global ocean tides: modern insights from FES2004. Ocean Dyn. 56, 394–415. https://doi.org/10.1007/s10236-006-0086-x.

Mao, X., Arnold, D., Girardin, V., Villiger, A., Jäggi, A., 2021. Dynamic GPS-based LEO orbit determination with 1 cm precision using the Bernese GNSS software. Adv Space Res 67 (2), 788–805. https://doi.org/10.1016/j.asr.2020.10.012.

Mao, X., Arnold, D., Kalarus, M., Padovan, S., Jäggi, A., 2023. GNSS-based precise orbit determination for maneuvering LEO satellites. GPS Sol 27, 147. https://doi.org/10.1007/s10291-023-01494-6.

Mayer-Gürr, T., Behzadpour, S., Eicker, A., Ellmer, M., Koch, B., Krauss, S., Pock, C., Rieser, D., Strasser, S., Süsser-Rechberger, B., Zehentner, N., Kvas, A., 2021. GROOPS: a software toolkit for gravity field recovery and GNSS processing. Comput. Geosci. 155. https://doi.org/10.1016/j.cageo.2021.104864 104864.

McCarthy, D.D., Petit, G. 2004. IERS Conventions (2003) (IERS Technical Note 32) Frankfurt am Main: Verlag des Bundesamts für Kartographie und Geodäsie, 127 pp., ISBN 3-89888-884-3 https://www.iers.org/IERS/EN/Publications/TechnicalNotes/tn32.html.

Montenbruck, O., Garcia-Fernández, M., Williams, J., 2006. Performance comparison of semicodeless GPS receivers for LEO satellites. GPS Solut 10 (4), 249–261. https://doi.org/10.1007/s10291-006-0025-9.

Montenbruck, O., Hackel, S., Jäggi, A., 2018. Precise orbit determination of the Sentinel-3A altimetry satellite using ambiguity-fixed GPS carrier phase observations. J Geod 92, 711–726. https://doi.org/10.1007/s00190-017-1090-2.

Montenbruck, O., Hackel, S., Wermuth, M., Zangerl, F., 2021. Sentinel-6A precise orbit determination using a combined GPS/GALILEO receiver. J Geod 95, 109. https://doi.org/10.1007/s00190-021-01563-z.

NASA, 2023a. GEODYN Software Package. Available at https://space-geodesy.nasa.gov/techniques/tools/GEODYN/GEODYN.html, last access: 5 Jan 2024.

NASA, 2023b. GIPSY-OASIS Jet Propulsion Laboratory. Available at: https://gipsy-oasis.jpl.nasa.gov, last access: 5 Jan 2024.

Pearlman, M.R., Noll, C.E., Pavlis, E.C., Lemoine, F.G., Combrink, L., Degnan, J.J., Kirchner, G., Schreiber, U., 2019. The ILRS: approaching 20 years and planning for the future. J Geod 93, 2161–2180. https://doi.org/10.1007/s00190-019-01241-1.

Peter, H., Springer, T., Otten, M., Fernández, J., Escobar, D., Féménias, P. 2015. Supporting Sentinels POD Service. Proceedings of Sentinel-3 for Science Workshop, June 2-5, 2015. Venice, Italy. ESA SP-734. https://sentinels.copernicus.eu/documents/d/sentinel/s34sci15_2015_supporting-sentinels-pod-service. Last access: 5 Jan 2024.

Peter, H., Berzosa, J., Fernández, M., Fernández, J., Féménias, P. 2021. Updates in the non-gravitational force modelling and orbit parametrization of the Copernicus Sentinel-1, -2, -3 satellites. Poster presented at 43rd COSPAR Scientific Assembly, 28 Jan – 4 Feb 2021, virtual meeting.

Peter, H., Jäggi, A., Fernández, J., Escobar, D., Ayuga, F., Arnold, D., Wermuth, M., Hackel, S., Otten, M., Simons, W., Visser, P., Hugentobler, U., Féménias, P., 2017. Sentinel-1A – first precise orbit determination results. Adv Space Res 60 (5), 879–892. https://doi.org/10.1016/j.asr.2017.05.034.

Peter, H., Fernández, J., Féménias, P., 2020. Copernicus Sentinel-1 satellites: sensitivity of antenna offset estimation to orbit and observation modelling. Adv Geosci 50, 87–100. https://doi.org/10.5194/adgeo-50-87-2020.

Peter, H., Meyer, U., Lasser, M., Jäggi, A., 2022. COST-G gravity field models for precise orbit determination of low earth orbiting satellites. Adv Space Res 69 (12), 4155–4168. https://doi.org/10.1016/j.asr.2022.04.005.

Petit, G., Luzum, B. 2010. IERS Conventions (2010) (IERS Technical Note 36) Frankfurt am Main: Verlag des Bundesamts für Kartographie und Geodäsie, 179 pp., ISBN 3-89888-989-6 https://www.iers.org/IERS/EN/Publications/TechnicalNotes/tn36.html.

Picone, J.M., Hedin, A.E., Drob, D.P., Aikin, A.C., 2002. NRLMSISE-00 empirical model of the atmosphere: statistical comparisons and scientific issues. J Geophys Res 107 (A12), 1468. https://doi.org/10.1029/2002JA009430.

Rebischung, P., Schmid, R. 2016. IGS14/igs14.atx: a new framework for the IGS products. In: AGU Fall Meeting, pp G41A-0998.

Rebischung, P. 2012. IGb08: an update on IGS08. IGSMAIL-6663, 24 Sep 2012. Available at https://lists.igs.org/pipermail/igsmail/2012/000497.html, last access: 5 Jan 2024.

Romero, I. 2020. RINEX The Receiver Independent Exchange Format Version 3.05. Available at https://files.igs.org/pub/data/format/rinex305.pdf, last access: 5 Jan 2024.

Roselló, J., Silvestrin, P., Weigand, R., d'Addio, S., Rodríguez, A.G., Risueño, G.L. 2012. Next generation of ESA's GNSS receivers for Earth observation satellites. In: 2012 6th ESA workshop on satellite navigation technologies (Navitec 2012) & European workshop on GNSS signals and signal processing. IEEE, pp 1–8. Available at http://microelectronics.esa.int/papers/Navitec12-AGGA4-Paper.pdf, last access 5 Jan 2024.

Rudenko, S., Dettmering, D., Esselborn, S., Schöne, T., Förste, C., Lemoine, J.M., Ablain, M., Alexandre, D., Neumayer, K.H., 2014. Influence of time variable geopotential models on precise orbits of altimetry satellites, global and regional mean sea level trends. Adv Space Res 54 (1), 92–118. https://doi.org/10.1016/j.asr.2014.03.010.

Rudenko, S., Dettmering, D., Zeitlhöfer, J., Alkahal, R., Upadhyay, D., Blossfeld, M., 2023. Radial orbit errors of contemporary altimetry satellite orbits. Surv. Geophys. 44, 705–737. https://doi.org/10.1007/s10712-022-09758-5.

Rudenko, S., König, R., Neumayer, K.-H., Raimondo, J.-C., Flechtner, F. 2011. Earth Parameter and Orbit System – Orbit Computation (EPOS-OC) software – a tool for space geodesy research at GFZ. Presentation at DORIS Analysis Working Group meeting (AWG) of the International DORIS Service, May 23-24, 2011, Paris, France. Available at https://ids-doris.org/images/documents/report/AWG201105/IDSAWG1105-Rudenko-EPOSsoftware.pdf, last access: 5 Jan 2024.

Saquet, E., Couhert, A., Peter, H., Arnold, D., Mercier, F., 2024. Millimeter accuracy SLR bias determination using independent multi-LEO DORIS and GPS-based precise orbits. Adv Space Res 73 (1), 304–316. https://doi.org/10.1016/j.asr.2023.07.014.

Savcenko, R., Bosch, W., Dettmering, D., Seitz, F., 2012. EOT11a - global Empirical Ocean tide model from multi-mission satellite altimetry, with links to model results. PANGAEA. https://doi.org/10.1594/PANGAEA.834232.

Springer, T., Dilssner, F., Escobar, D., Flohrer, C., Otten, M., Svehla, D., Zandbergen, R. 2011. NAPEOS: The ESA/ESOC Tool for Space Geodesy. Geophysical Research Abstracts. Vol.13, EGU2011-8287. Available at https://meetingorganizer.copernicus.org/EGU2011/EGU2011-8287.pdf, last access: 5 Jan 2024.

Stark, H.R., Möller, H.L., Courrèges-Lacoste, G.B., Koopman, R., Mezzasoma, S., Veihelmann, B. 2020. The Sentinel-4 Mission, its Components and Implementation. Available at https://www-cdn.eumetsat.int/files/2020-04/pdf_conf_p_s1_10_stark_v.pdf, last access: 5 Jan 2024.

Torres, R., Snoeij, P., Geudtner, D., Bibby, D., Davidson, M., Attema, E., Potin, P., Rommen, B., Floury, N., Brown, M., Traver, I., Deghaye, P., Duesmann, B., Rosich, B., Miranda, N., Bruno, C., L'Abbate, M., Croci, R., Pietropaolo, A., Huchler, M., Rostan, F., 2012. GMES Sentinel-1 mission. Remote Sens Environ 120, 9–24. https://doi.org/10.1016/j.rse.2011.05.028.

van den IJssel, J., Encarnação, J., Doornbos, E., Visser, P., 2015. Precise science orbits for the SWARM satellite constellation. Adv Space Res 56 (6), 1042–1055. https://doi.org/10.1016/j.asr.2015.06.002.

Veefkind, J.P., Aben, I., McMullan, K., Förster, H., de Vries, J., Otter, G., Claas, J., Eskes, H.J., de Haan, J.F., Kleipool, Q., van Weele, M., Hasekamp, O., Hoogeveen, R., Landgraf, J., Snel, R., Tol, P., Ingmann, P., Voors, R., Kruizinga, B., Vink, R., Visser, H., Levelt, P. F., 2012. TROPOMI on the ESA Sentinel-5 precursor: a GMES mission for global observations of the atmospheric composition for climate, air quality and ozone layer applications. Remote Sens Environ 120, 70–83. https://doi.org/10.1016/j.rse.2011.09.027.

Villiger, A. 2022. Upcoming switch to IGS20/igs20.atx and repro3 standards. IGSMAIL-8238, 26 July 2022. Available at https://lists.igs.org/pipermail/igsmail/2022/008234.html, last access: 5 Jan 2024.

Visser, P.N.A.M., van den IJssel, J., Van Helleputte, T., Bock, H., Jäggi, A., Beutler, G., Švehla, D., Hugentobler, U., Heinze, M., 2009. Orbit determination for the GOCE satellite. Adv Space Res 43 (5), 760–768. https://doi.org/10.1016/j.asr.2008.09.016.

Wermuth, M., Montenbruck, O., Van Helleputte, T. 2010. GPS high precision orbit determination software tools (GHOST). In: 4th International conference on astrodynamics tools and techniques, Madrid, Spain, 3–6 May, 2010.

Woo, K.T., 2000. Optimum semicodeless carrier-phase tracking of L2. Navigation 47 (2), 82–99. https://doi.org/10.1002/j.2161-4296.2000.tb00204.x.

Wu, S.C., Yunck, T.P., Thornton, C.L., 1991. Reduced-dynamic technique for precise orbit determination of low earth satellites. J Guid Control Dyn 14 (1), 24–30. https://doi.org/10.2514/3.20600.

Zangerl, F., Griesauer, F., Sust, M., Montenbruck, O., Buchert, B., Garcia, A. 2014. SWARM GPS precise orbit determination receiver initial in-orbit performance evaluation. In: 27th International Technical Meeting of the Satellite Division of the Institute of Navigation, ION GNSS 2014. Vol.2, 1459-1468.

Zumberge, J.F., Heflin, M.B., Jefferson, D.C., Watkins, M.M., Webb, F. H., 1997. Precise point positioning for the efficient and robust analysis of GPS data from large networks. J Geophys Res 102 (B3), 5005–5017. https://doi.org/10.1029/96JB03860.